COMPUTATIONAL TECHNIQUES IN INFRASONIC WAVEFORM SYNTHESIS

A THESIS

Presented to

The Faculty of the Division of Graduate

Studies and Research

by

Christopher Kapper

In Partial Fulfillment

of the Requirements for the Degree

Master of Science in Mechanical Engineering

Georgia Institute of Technology

December, 1974

COMPUTATIONAL TECHNIQUES IN INFRASONIC

WAVEFORM SYNTHESIS

Approved:

A. D. Pierce, Chairman

P. V. Desai

C. G. Justus

G. L. Maynard

Date approved by Chairman: Nov. 11, 1974

ACKNOWLEDGMENTS

The author wishes to express his most sincere appreciation to his advisor, Dr. Allan Pierce, for the opportunity to work on this problem and for his invaluable guidance, patience, and encouragement in the completion of this work. Appreciation is extended to Dr. C. G. Justus, Dr. G. L. Maynard and Dr. P. V. Desai for their review and service on the reading committee. This work was sponsored by the U. S. Air Force Cambridge Research Laboratories, Office of Aerospace Research.

TABLE OF CONTENTS

LIST OF ILLUSTRATIONS

SUMMARY

This thesis is concerned with two major theoretical and programming modifications to the digital computer program INFRASONIC WAVEFORMS for the synthesization of acoustic-gravity pressure waveforms generated by large explosions in the atmosphere.

The first modification involves the extension of the guided mode approximation for pressure waveforms in the atmosphere into leaking mode regions and a consequent search for the imaginary part of the complex horizontal wave number. Particular results include a plot of phase velocity versus angular frequency showing the extension of the normal mode dispersion function into a leaky mode region for a multilayer atmosphere and a report on the search for the imaginary part of the complex horizontal wave number of a leaky mode for a two layer atmosphere.

The second modification involves the extension of the systhesis of acoustic-gravity pressure waveforms to distances beyond the antipode. A phase shift is noted for waves passing through the antipode and a comparison of pre and post antipodal waveforms is presented.

CHAPTER I

INTRODUCTION

Since the early 1960's extensive efforts have been devoted to the development of an accurate digital computer program for the theoretical prediction of acoustic-gravity pressure waveforms generated by nuclear explosions in the atmosphere. One notable result of such efforts is the digital computer program INFRASONIC WAVEFORMS[1] written jointly by A. D. Pierce and J. W. Posey, a version of whose complete deck listing (in Fortran IV for the IBM 360 system) appears in the Air Force Cambridge Research Laboratories report number AFCRL-70-0134. This program allows a theoretical prediction of the acoustic pressure waveform which would be recorded at large horizontal distances (500 to 19,000 km) from a low to moderate altitude thermonuclear explosion in the atmosphere. The atmosphere is considered to be perfectly stratified and comprised of as many as 100 layers, each having constant temperature and wind velocity. Each layer may have different values of temperature, wind-velocity magnitude, and wind-velocity direction. By supplying the appropriate atmospheric data, one can, in principle, achieve a reasonable model of the atmosphere. Other inputs to the program include the estimated yield of the source explosion,

its height, the height of the observer above ground, and the distance from source to the observation point. The output includes a table of the sign of the eigenmode dispersion function for an array of points in the V_p (phase velocity) versus ω (angular velocity) plane, a tabulation of V_p versus ω values for each mode so depicted (i.e., the lines in the V_p versus ω plane where the dispersion function change sign), and a Calcomp plot of modal and total waveforms on a common time axis and with a common pressure scale.

Until recently, the computer program INFRASONIC WAVEFORMS was restricted to the inclusion of only fully ducted modes (real phase velocity) in the modal approximation for the synthesis of pressure waveforms and was also restricted to observer distances less than halfway around the globe from the explosion. Both of these along with a number of other restrictions are discussed in the recent report by Pierce, Moo, and Posey[2] and a possible method of removing the second restriction is also described there. In the present work, additional theoretical developments and computational techniques are described which will remove the first restriction. Also, a detailed exposition is given of the theoretical basis and numerical implications of the previously suggested method for synthesizing antipodal waveforms.

CHAPTER II

EXTENSION OF INFRASONIC WAVEFORMS TO INCLUDE WEAKLY LEAKING MODES

Prior theoretical formulations and computational techniques for the prediction of pressure waveforms generated by large explosions in the atmosphere have considered only fully ducted modes. In this chapter, a technique for including weakly leaking guided modes in concert with fully ducted modes is considered. Modification of previous theory includes the extension of the boundary condition at the upper halfspace of the atmosphere to allow a complex horizontal wave number. A major alteration to the computer program INFRASONIC WAVEFORMS is developed and consists of the extension of certain previously truncated modes to lower frequencies. The significance of the weakly leaking modes is also discussed.

2.1 Theoretical Considerations for the Inclusion of Weakly Leaking Modes

The present theory on which this chapter is based consists of the guided mode solution for the multilayer approximation for wave propagation in the atmosphere. The actual atmosphere is replaced by a multilayer model comprised of a discrete number of layers each having constant temperature

and wind velocity.[1] This layered model facilitates the calculation of the desired parameters describing the wave propagation in the actual atmosphere. The multilayer atmosphere is bounded on the top by an isothermal halfspace with constant winds and on the bottom by a rigid earth.

The wave propagation is governed by the linearized equations of hydrodynamics for air in the absence of viscosity and thermal conductivity. As previously given by Pierce (1967)[3] and by Pierce, Posey, and Iliff[4] the linearized hydrodynamic equations are written as

$$\rho_o[D_t\vec{u}+(\vec{u}\cdot\nabla)\vec{v}] = -\vec{\nabla}_p - g\rho\vec{e}_z \tag{2.1a}$$

$$D_t\rho+\vec{u}\cdot\vec{\nabla}\rho_o + \rho_o\vec{\nabla}\cdot\vec{u} = 0 \tag{2.1b}$$

$$(D_t p+\vec{u}\cdot\vec{\nabla}p_o) - c^2(D_t\rho+\vec{u}\cdot\vec{\nabla}\rho_o) = 4\pi c^2 f_E(t)\delta(\vec{r}-\vec{r}_o) \tag{2.1c}$$

where

$$D_t = (\partial/\partial t)+\vec{v}\cdot\vec{\nabla} \tag{2.2}$$

is the time derivative corresponding to an observer moving with the ambient wind. The above equations represent a set

of coupled partial differential equations for the deviations p, ρ, $\vec{u}$ of the pressure, density, and fluid velocity from their respective ambient values of p_o, ρ_o, and $\vec{v}$. The source term on the right hand side of Eq. (2.1c) is as previously described by Pierce, Posey, and Iliff.[4] The speed of sound c, in a homogeneous atmosphere with neglection of gravity, can be written as

$$c = (\gamma p_o/\rho_o)^{1/2} \tag{2.3}$$

In the preceding equations the acceleration of gravity, the unit vector in the vertical direction, and the ratio of specific heats in air are respectively represented by the quantities g, $\vec{e}_z$, and γ. Also in the equations mentioned above the ambient or zeroth order values of pressure, density, and fluid velocity (i.e., p_o, ρ_o, and $\vec{v}$) are assumed independent of time t and the horizontal coordinates x and y. In conjunction with these assumptions the ambient wind velocity $\vec{v}$ is considered to be entirely horizontal. However, all ambient variables may vary arbitrarily with height z. The quantities p_o and ρ_o are constrained to vary with height according to the hydrostatic equation

$$dp_o/dz = -g\rho_o \tag{2.4}$$

and the ideal gas law.

In the digital computer program INFRASONIC WAVEFORMS the specific heat ratio is taken as $\gamma = 1.4$ and the acceleration of gravity g is taken to be constant with height and equal to .0098 km/sec^2. Based on the above equations, it has been shown by Pierce and Posey[1] (with the earth curvature correction as discussed by Pierce, Posey, and Iliff[4]) that the far field waveforms may be approximately expressed in the form

$$P = [(r/r_e)/|\sin(r/r_e)|]^{1/2} \operatorname*{Re}_{[\lim \varepsilon \to 0]} \int_{o+i\varepsilon}^{\infty+i\varepsilon} e^{-i\omega t} \hat{f}_E(\omega) L d\omega \qquad (2.5)$$

where

$$L = \int_{-\infty}^{\infty} (2\pi k/r)^{1/2} e^{i(kr-\pi/4)} \hat{p}(\omega, k, \theta) e^{i\alpha} dk \qquad (2.6)$$

Here the phase of $k^{1/2}$ along the negative axis is understood to be $\pi/2$. The quantity r is understood to represent the great circle distance along the earth's surface from source to microphone, while θ represents the azimuth angle of the observer location, reckoned counterclockwise about a pole passing through the source location. The quantity $\hat{f}_E(\omega)$ is the Fourier transform of the source function $f_E(t)$, i.e.,

$$\hat{f}_e(\omega) = (2\pi)^{-1} \int_{-\infty}^{\infty} f_E(t) e^{i\omega t} dt \qquad (2.7)$$

In regards to the other symbols which appear above, ε is any arbitrary small but non-zero real number, r_e is the radius of the earth and, for real k, α is 0 if $r<\pi r_e$; $\pi/2$ if $2\pi r_e>r>\pi r_e$ (antipodal arrivals), etc., while $\hat{p}(w,k,\theta)$ is defined below. The expression (2.5) is understood to apply both for arrivals not having yet or already having traveled halfway around the globe, but not to apply in the immediate vicinity of the antipodes ($r = \pi r_e$).

The remaining quantity $\hat{p}(w,k,\theta)$ is given by

$$\hat{p} = - \left[\frac{\rho_o(z)}{\rho_o(z_o)}\right]^{1/2} \frac{1}{\pi\Omega(z_o)} \frac{\psi(z,z_o)}{\Phi_{1u}(0)\Phi_{2\ell}(0)} \tag{2.8}$$

where

$$\psi(z,z_o) = c(z_o)c(z)\Phi_{2u}(z_o)[\Phi_{2\ell}(z)-gc^{-2}(z)\Phi_{1\ell}(z)]$$

$$\text{if } z_o>z \tag{2.9a}$$

$$= c(z_o)c(z)\Phi_{2\ell}(z_o)[\Phi_{2u}(z)-gc^{-2}(z)\Phi_{1u}(z)]$$

$$\text{if } z_o<z \tag{2.9b}$$

and

$$\Omega(z) = \omega-\vec{k}\cdot\vec{v}(z) \tag{2.10}$$

Here $\rho_o(z)$ and $\rho_o(z_o)$ represent the ambient densities at the observer height z (above the earth's surface) and at the burst height z_o, respectively. The other quantities Φ_{1u}, Φ_{2u} or $\Phi_{1\ell}$, $\Phi_{2\ell}$ represent solution pairs to the residual equations (defined below) which satisfy upper (u) and lower (ℓ) boundary conditions, respectively.

The form of the residual equations in matrix notation is

$$d/dz \begin{bmatrix} \Phi_1 \\ \Phi_2 \end{bmatrix} = \begin{bmatrix} A_{11} & A_{12} \\ A_{21} & A_{22} \end{bmatrix} \begin{bmatrix} \Phi_1 \\ \Phi_2 \end{bmatrix} \tag{2.11}$$

where

$$A_{11} = g(k^2/\Omega^2) - \gamma g/2c^2) \tag{2.12a}$$

$$A_{12} = 1-(c^2k^2/\Omega^2) \tag{2.12b}$$

$$A_{21} = g^2k^2/(\Omega^2c^2) - \Omega^2/c^2 \tag{2.12c}$$

$$A_{22} = -A_{11}$$

with

$$\Omega = \omega - k_x v_x - k_y v_y \tag{2.13}$$

$$k^2 = k_x^2 + k_y^2 \tag{2.14}$$

In the above expressions $k_x = k\cos(\theta)$ and $k_y = k\sin(\theta)$ are the horizontal wave number vector components, v_x and v_y are the ambient horizontal wind components, and ω represents angular frequency. It can be seen from the coefficients of Eqs. (2.12) that none depend explicitly on the derivatives of sound speed or wind speed with respect to height. This implies that Φ_1 and Φ_2 are continuous with z even when c and $\vec{v}$ are discontinuous. The quantities Φ_1 and Φ_2 are functions of z, but not of x, y, or t. The matrix [A] is constant for any given layer and for the upper halfspace and is computed by an existing subroutine called AAAA in INFRASONIC WAVEFORMS.

The solution pair $\Phi_{1\ell}(z)$, $\Phi_{2\ell}(z)$ satisfy the boundary conditions that $\Phi_{1\ell}(0) = 0$ corresponding to the requirement that $u_z = 0$ at the rigid earth, $z = 0$. The other pair $\Phi_{1u}(z)$, $\Phi_{2u}(z)$ satisfy the condition that, in the upper halfspace, $z > z_T$,

$$\begin{bmatrix} \Phi_1 \\ \Phi_2 \end{bmatrix} = D \begin{bmatrix} -A_{12} \\ A_{11}+G \end{bmatrix} e^{-G(z-z_T)} \tag{2.15}$$

where

$$G = (A_{11}^{\ 2} + A_{12}A_{21})^{1/2} \tag{2.16}$$

where D is any arbitrary constant and z_T is the bottom of the upper halfspace. Here the ambiguity intrinsic to taking the square root is resolved by placing branch lines in the complex k plane which terminate in branch points at which $G = 0$ or at ∞ and by specifying the phase of G at a single point. (This is discussed further below.)

The values of Φ_1 and Φ_2 (u or ℓ) at any height z_2 may be expressed in terms of those at height z_1 by a transmission matrix $[R(z_2, z_1)]$ such that

$$\begin{bmatrix} \Phi_1 \\ \Phi_2 \end{bmatrix}_{z=z_2} = [R(z_2,z_1)] \begin{bmatrix} \Phi_1 \\ \Phi_2 \end{bmatrix} \tag{2.17}$$

where $[R(z_2,z_1)]$ considered as a function of z_2 satisfies the residual equations and reduces to the identity matrix when $z_2 = z_1$. In the event that $z_2 = 0$, $z_1 = z_T$, the matrix [R] is computed by an existing subroutine called RRRR in INFRASONIC WAVEFORMS. One may note also that the fact that the trace of [A] is 0 implies that the determinant of [R] be 1.

In terms of the matrix $[R(z_2,z_1)]$ defined above, the quantity β which appears in Eq. (2.8) may be rewritten as

$$\hat{p} = - \left[\frac{\rho_o(z)}{\rho_o(z_o)}\right]^{1/2} \frac{c(z)c(z_o)}{\pi\Omega(z_o)} \frac{MN}{[\text{Dispersion Function}]} \quad (2.18)$$

where, for $z_o > z$,

$$M = A_{12}R_{21}(z_o,z_T) - (A_{11}+G)R_{22}(z_o,z_T) \quad (2.19a)$$

$$N = R_{22}(z,0) - gc^{-2}(z)R_{12}(z,0) \quad (2.19b)$$

while, for $z_o < z$

$$M = R_{22}(z_o,0) \quad (2.20a)$$

$$N = A_{12}[R_{21}(z,z_T) - gc^{-2}(z)R_{11}(z,z_T)]$$

$$-(A_{11}+G)[R_{22}(z,z_T) - gc^{-2}(z)R_{12}(z,z_T)] \quad (2.20b)$$

The dispersion function is given by

$$[\text{Dispersion Function}] = A_{12}R_{11}(\theta,z_T) - (A_{11}+G)R_{12}(0,z_T) \quad (2.21)$$

In previous reports this has been referred to as the normal mode dispersion function. However, for various reasons, it has been concluded that the adjective normal may be misleading, so in this paper, the function is referred to as

the eigenmode dispersion function.

The previous technique for evaluating the k integration in Eq. (2.6) was to imagine the contour integration along the real axis to be replaced by one along a contour encircling all poles in the upper half plane in the counterclockwise sense plus branch line integrals which follow along successive sides of each branch cut in the upper half plane in the counterclockwise sense. The branch line integrations were discarded and the integration around the poles was evaluated by Cauchy's residue theorem, such that

$$L = 2\pi i \sum_n \left(\frac{2\pi k_n}{r}\right)^{1/2} e^{i(k_n r - \pi/4)} e^{i\alpha} (\mathrm{Res})_n \qquad (2.22)$$

where $(\mathrm{Res})_n$ was the residue of $\hat{p}$ at a pole k_n and it was understood that only those poles should be included which lay above the real axis when $\varepsilon>0$. Moreover, in the actual computation, one included only those poles which were on the real axis in the limit of $\varepsilon>0$. Loosely speaking therefore, all leaking modes were excluded. However, one may also note that the presence of any given pole depends somewhat on the choice of the branch line location. (These are somewhat variable although the branch points themselves are not.) The tacit selection which was adopted was that G should have a positive real part everywhere in the upper k plane (in the limit $\varepsilon>0$) and that, along the real axis, whenever G^2 was

real and positive, it was understood that G should be real and positive. To a certain extent, this made good sense the resulting eigensolutions would then always die out at large z. (See Eq. 2.15.) However, one should note that, in a strict mathematical sense, the total integral (2.6) should be independent of just where the branch lines are placed, providing no branch line crosses the real axis.

The poles of interest, in any event, should be those values of k at which the eigenmode dispersion function (2.21) vanishes, i.e., where

$$F(\omega,\theta,k) = R_{11}A_{12}^{U}-R_{12}(G^{U}+A_{11}^{U}) = 0 \qquad (2.23)$$

for some selection of the branch lines defining the phase of G^{U}. Here the superscript U implies that the values of the designated quantities are those appropriate to the upper halfspace. Also, for brevity, one can write R_{11} and R_{12} for the matrix elements $R_{11}(0,z_T)$, $R_{12}(0,z_T)$. The eigenmode dispersion function is also a function of the height profiles of c, v_x, and v_y. During any computational synthesis of a single generated waveform, these profiles remain unchanged so they are not included in the argument list of the eigenmode dispersion function $F(\omega,\theta,k)$. When $F(\omega,\theta,k) = 0$ for a real value of k in the limit that ω is real and when the corresponding value of G^{U} is real and positive, the corresponding solution of the residual equations

satisfies both upper and lower boundary conditions and represents a guided mode. The magnitude of the horizontal phase velocity of such a wave is given by

$$V_p = (\omega^2/k^2)^{1/2} \tag{2.24a}$$

The angle θ defines the phase velocity direction by use of the expressions

$$k_x = k \cos\theta \tag{2.24b}$$

$$k_y = k \sin\theta \tag{2.24c}$$

where k is the positive square root of k^2.

In the present version of the digital computer program INFRASONIC WAVEFORMS the roots of the eigenmode dispersion function are found numerically but only for the case when G^2 is positive and k is real and positive. For a fixed value of θ, the eigenmode dispersion function can be considered as a function of phase velocity V_p and angular frequency ω. Finding the roots of $F_\theta(\omega,k) = 0$ for a fixed θ is accomplished by tabulating a V_p versus ω array between predetermined maximum and minimum values of the former quantities. When the computer is incrementing through the ω range, it is also (for each value of ω) incrementing through the prescribed V_p range. For each point in the V_p

versus ω array the value of $F_\theta(\omega,V_p)$, and hence its sign, is computed. Eventually the sign of $F_\theta(\omega,V_p)$, either + or -, is printed out in an array of V_p versus ω corresponding to those values of V_p and ω that determined it. The sign changes that appear in the array indicate the curves of the eigenmodes to zeroth order. Such curves are called dispersion curves. After a check and an expanded array is produced to resolve apparently intersecting modes (see Fig. 1), a numerical iteration technique is used to determine the roots of the eigenmodes. The computer follows the curves indicated by the sign changes calculating the roots of $F_\theta(\omega,V_p)$ using the array values as zeroth order starting points.

However, in the previous version of the computer program, when G^2 is negative in the upper halfspace, the eigenmode dispersion function is not defined. In this case the previous theory then assumes that $F_\theta(\omega,V_p)$ does not exist for those values of V_p and ω. The computer will then print an X in the array at the appropriate array points where this condition occurs. The extension of the theory to improve the handling of such cases is the concern of this chapter.

2.2 Proposed Computational Technique for the Inclusion of Leaky Modes

In order to avoid the difficulties mentioned in the previous section and in particular, to avoid the apparently

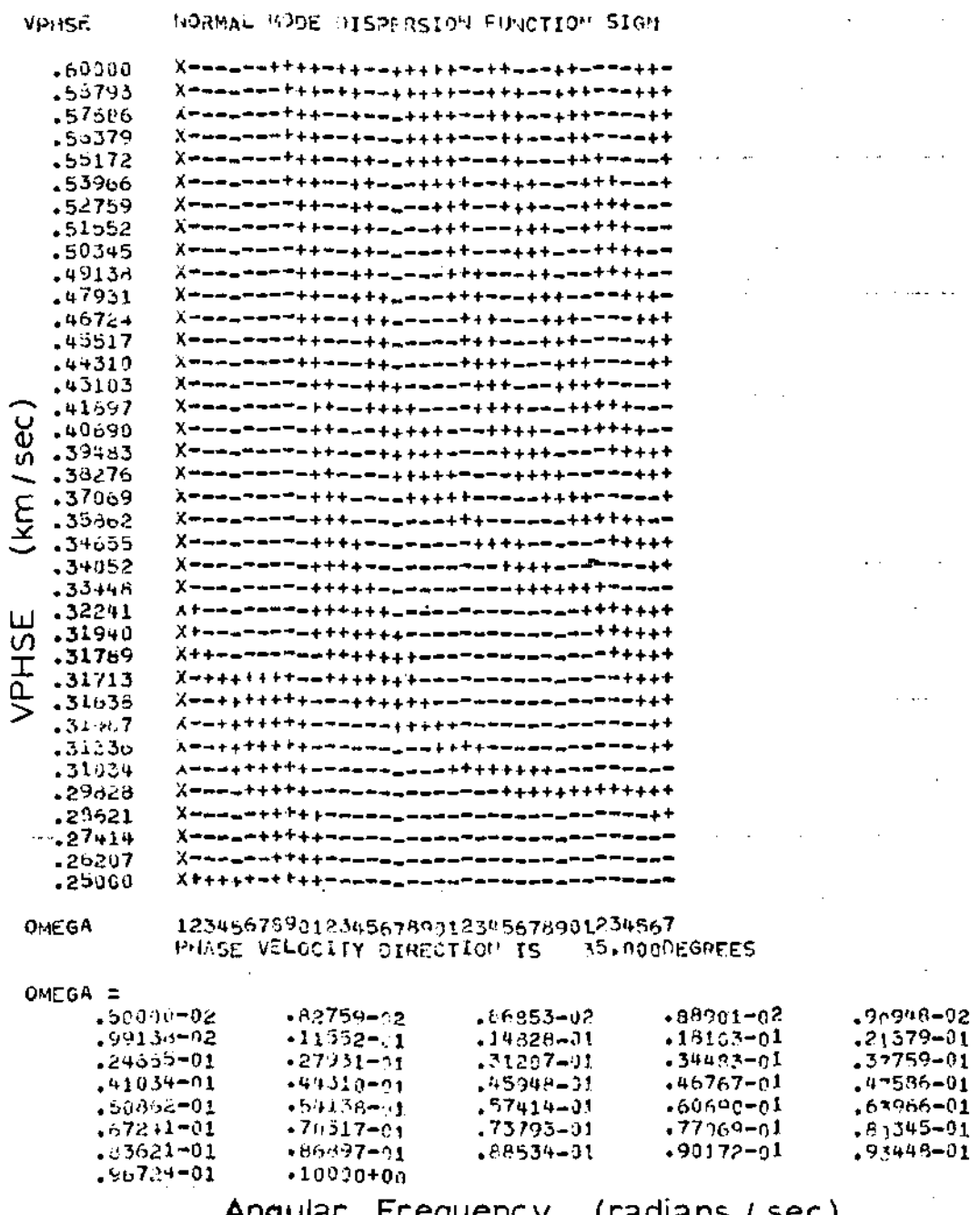

Figure 1. Sign of the Eigenmode Dispersion Function for a 32 Layer Atmosphere. Source is a 10 megaton explosion.

artificial low frequency truncation of certain modes, it is sought to devise a somewhat improved computational scheme than that presented by Pierce and Posey.[1] The tentative scheme so devised is briefly outlined here.

First, branch line integrals are still formally neglected. However, in order to minimize the relative contribution of such branch line integrals it is assumed that the branch lines be placed such that there are no poles on either branch in the vicinity of a branch line. This then requires that the sum in Eq. (2.22) may include some contributions from poles not necessarily corresponding to Re $G>0$.

Secondly, we include only those poles which correspond either to real guided modes or else to the low frequency extension of modes which at higher frequencies were real and guided. In other words, we avoid the computational difficulties of searching for all possible complex roots irrespective of branch of the eigenmode dispersion function and then deciding where to place branch lines and of what poles to include. The concept adopted is that the same modes exist at all frequencies but at some frequencies a given mode may be leaky and possibly correspond to a pole on a different branch of G.

In regards to actual computation of the location of the poles of interest, some exploratory computations (described further in the next section) have indicated that the roots of interest of the eigenmode dispersion function

are very close in actual value to what would be expected if one set G = 0 identically, i.e., if one replaced F by $F^\circ(\omega,k)$ where

$$F^\circ(\omega,k) = A^U_{12}R_{11} - A^U_{11}R_{12} \tag{2.25}$$

Furthermore, the roots of interest of $F^\circ(\omega,k) = 0$ are those which, for real positive ω, correspond to real positive values of k and phase velocity. The roots of this equation are denoted by $k^o_n(\omega)$.

The above observation suggests that the zero order roots of the eigenmode dispersion function may be easily obtained with only a slight modification to the existing program. Figure 2 shows the resulting array for a two layer atmosphere using the results above. Insofar as the amplitudes are concerned, it would appear to be sufficient to compute the residue $(Res)_n$ in Eq. (2.22) as if the demoninator in Eq. (2.18) were just F°, i.e., $(Res)_n$ is as given by Eq. (2.18) with k everywhere replaced by k^o_n, only with the denominator F replaced by $\partial F^\circ/\partial k$ evaluated at $k = k^o_n$.

It may, however, be insufficient to identically set $k_n = k^o_n$ in the exponential factor $\exp(ik_nr)$ which appears in Eq. (2.22) since we are interested in the case of relatively large r and a small error in k_n could lead to a large error in the exponential. Consequently, we have endeavored to devise a scheme for calculating a correction

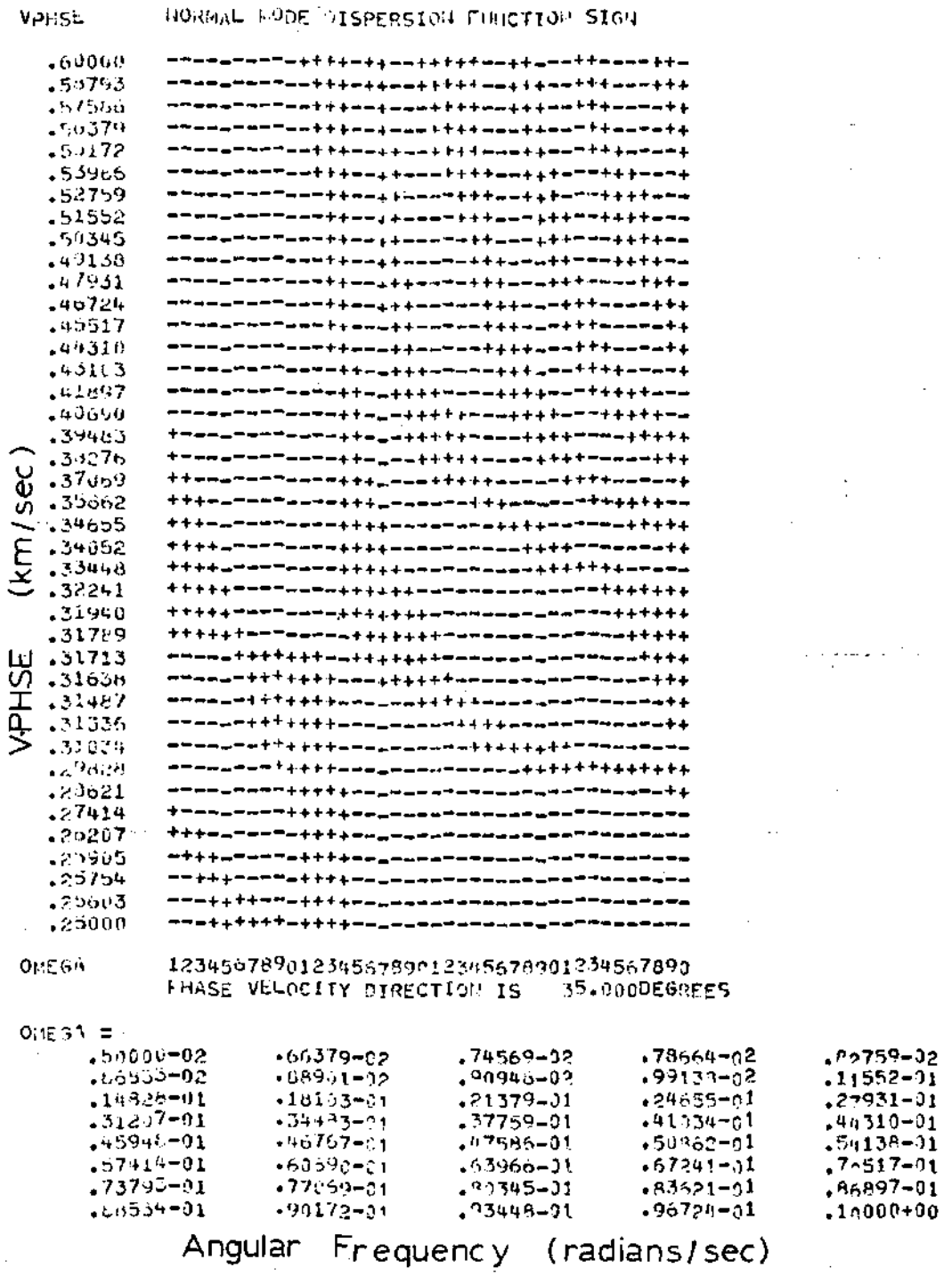

Figure 2. Sign of the Extended Eigenmode Dispersion Function for a 32 Layer Atmosphere. Source is a 10 megaton explosion.

to the value k_n.

In the event that $G^2>0$ at $k = k_n^o$ it is generally the case that a reasonably accurate solution (yielding a real root) to $F(\omega,k) = 0$ may be found by the numerical method already incorporated in the earlier version of INFRASONIC WAVEFORMS. Problems arise with the method if $G^2<0$ or very close to 0. In this event, it would appear appropriate to write the equation $F = 0$ in the appropriate form

$$(\partial F^\circ/\partial k)_o(k-k^\circ) \pm Q_o[k_B-k]^{1/2} = 0 \qquad (2.26)$$

where k° is a root of $F^\circ = 0$ and $(\partial F^\circ/\partial k)_o$ is the derivative of F° at that root. Thus the first term of Eq. (2.26) is the value of F° in the vicinity of one of its zeros. The second term accordingly represents an approximation to $-R_{12}G^U$. Specifically, we note that, in the cases of interest, $G^2 = 0$ at a value k_B (branch point) of k and $G^2>0$ for $k<k_B$. Consequently, one could write $-R_{12}G$ as $Q[k_B-k]^{1/2}$ where

$$Q = -R_{12}G/[k_B-k]^{1/2} \qquad (2.27)$$

should be real and have no branch points along the positive real axis. In Eq. (2.26) we have approximated Q by Q_o which would be its value evaluated at $k = k^\circ$. The $\pm$ sign in Eq. (2.26) implies that we may be seeking roots on either

branch. The reason that we do not set $k = k^\circ$ in the radical $[k_B-k]^{1/2}$ is that we anticipate that in some cases of interest k° may be very close to k_B.

Equation (2.26) may alternately be written as

$$\Delta k \pm \varepsilon[k_B-k^\circ-\Delta k]^{1/2} = 0 \tag{2.28}$$

where $\Delta k = k-k^\circ$ and

$$\varepsilon = Q_o/(\partial F^\circ/\partial k)_o \tag{2.29}$$

The solutions to the above are easily found to be

$$\Delta k = -(\varepsilon^2/2) \pm [(\varepsilon^4/4) + \varepsilon^2(k_B-k^\circ)]^{1/2} \tag{2.30}$$

For $k_B-k^\circ>-\varepsilon^2/4$ these two roots are real, while if $k_B-k^\circ<-\varepsilon^2/4$ the roots are complex. In the latter case, one selects only that root which lies in the upper half plane (i.e., such that the imaginary part of k is positive). This is consistent with the nature of our assumed contour deformation and, furthermore, gives the physically meaningful result that e^{ikr} should decrease in magnitude at large r.

If the two roots are real the one selected should be that which lies above the real axis when ω has a small positive part, i.e., such that

$$\partial(k^{\circ}+\Delta k)/\partial\omega>0 \qquad (2.31)$$

Presumably, only one of the two roots will satisfy this condition. Also this root should have a continuous trajectory in the k versus ω plane with variable real ω and should match onto the dispersion curve found by the numerical method presently utilized in INFRASONIC WAVEFORMS. The latter would imply that the sign in Eq. (2.30) should be the same as the sign of $-\varepsilon$.

2.3 Suggested Modifications to INFRASONIC WAVEFORMS

Applying the theory presented in the preceding sections to the digital computer program INFRASONIC WAVEFORMS involves some modification of existing subroutines and addition of new subroutines. At the time of this writing not all of the required modifications have been implemented. However, the following gives a detailed guide of how the implementation may proceed.

Among the necessary modifications are those involving the subroutine NMDFN which determines the value of the eigenmode dispersion function and hence its sign. This is done for given angular frequency OMEGA, phase velocity magnitude VPHSE, and phase velocity direction THETK. In computer nomenclature FPP is defined as representing the eigenmode dispersion function. In subroutine NMDFN the value

for G^2 is computed. In the unmodified version, if G^2 is negative, the subroutine returns for such values of OMEGA and VPHSE a message saying that FPP does not exist. This is subsequently (by other subroutines) recognized by the printing of an X in the V_p versus ω array of eigenmode dispersion function signs. In the modified version if $G^2<0$, a real value of FPP is computed by simply ignoring the term $-R_{12}G$ in the definition of F. In other words, the zeroth order value F° is computed. This implies that, at least formally, the eigenmode dispersion function will always exist. The resulting V_p versus ω array will then contain either a plus or minus sign where previously X's were printed. This will also allow the calculation of the zeroth order roots of FPP to be extended to lower frequencies. All that is required for this extension is to delete line 128 in NMDFN

```
126     C GUSQ IS LESS THAN ZERO
127           L=-1
128           RETURN          (Delete)
129     C
130     C GUSQ IS GREATER THAN ZERO
```

and to add the following lines after line 127

```
128     C ZEROTH ORDER APPROXIMATION FOR FPP
129     C GU=0.0 AND GUSQ = 0.0
130           GUSQ=0.0
131           GO TO 11
```

In the above GUSQ is G^2 and GU is G.

To calculate the corrected roots (which in general are complex) a subroutine COMPK is added. This is called in the main program by inserting the following statements

```
C CONTINUING WITH KWOP .GE. 0 FROM 308
  320 CALL COMPK(MDFND,KST,KFIN,OMMOD,UPMOD,THETK,CKI)
      IF (NPRNT .LE. 0) GO TO 350
```

Note that the zeroth order dispersion curves are inputs to COMPK while other inputs come through COMMON. The subroutine operates on these values and returns improved dispersion curves plus the corresponding imaginary part CKI of k for each tabulated point. Three subroutines written by A. D. Pierce while at AVCO[5] hitherto not included in INFRASONIC WAVEFORMS are called in COMPK to facilitate computation of derivatives. The three subroutines were updated and their deck listings appear in Appendix A along with a short introduction to each. All that need be stated here is that subroutine DADQR calculates the two-by-two matrices DADKX and DADKY which represent the derivatives of the matrix [A] with respect to the horizontal wave number components k_x and k_y. Subroutine DRDQR calculates the corresponding derivatives DRDKX and DRDKY of the matrix $[R(0,z_T)]$. A third subroutine DMDQR called by DRDQR calculates the corresponding derivatives for the single layer transmission matrix [M].

COMPK goes successively through each previously

tabulated point on each dispersion curve. In each case it first calculates GUSQ. If this is positive no corrections are made and the corresponding value of CKI is returned as 0. If GUSQ is negative the procedure outlined in Eqs. (2.26-2.31) is followed. First the value k_B is calculated. This is done approximately by simply assuming that GUSQ is linearly proportional to k_B-k. Thus one sets

$$k_B = k°-G^2/(dG^2/dk) \tag{2.32}$$

where k° = OMEGA/VPHSE, VPHSE being the previously computed zeroth order approximation to the phase velocity. The derivative dG^2/dk is computed by first calling DADQR for atmospheric values appropriate to the upper halfspace and then using Eq. (2.16), the derivative being

$$dG^2/dk = 2A_{11}(dA_{11}/dk) + A_{12}(dA_{21}/dk) + A_{21}(dA_{12}/dk) \tag{2.33}$$

where

$$d/dk = (\partial/\partial k_x)\cos\theta_k + (\partial/\partial k_y)\sin\theta_k \tag{2.34}$$

In a similar manner DRDQR and DADQR are used to evaluate the derivative $\partial F°/\partial k$. The parameter ε (EPSI) is then computed from Eqs. (2.27) and (2.29). If $k_B-k°>-\varepsilon^2/2$, the corrected value of k° is computed from Eq. (2.30) with

the sign before the radical being that of $-\varepsilon$. The old value of the phase velocity is then replaced by $\omega/(k^\circ+\Delta k)$. CKI is set to zero.

If $k_B-k^\circ<-\varepsilon^2/2$, then the new value of VPHSE is $\omega/(k^\circ-\varepsilon^2/2)$ while CKI = $[-\varepsilon^4/4-\varepsilon^2(k_B-k^\circ)]$. One pitfall in this method is the possibility that $k^\circ-\varepsilon^2/2$ could be negative. This is never anticipated as happening, but should it happen, we simply let VPHSE equal a very large value (10^6).

With regards to computation of amplitudes we have not yet revised the program to evaluate $(Res)_n$ which appears in Eq. (2.22). However, no difficulties are anticipated in doing this. In particular, it is planned to write a new subroutine which does this. Note that the derivative $\partial F^\circ/\partial k$ which appears in the denominator of $(Res)_n$ can easily be evaluated by use of the subroutine DRDQR and DADQR.

CHAPTER III

STUDY OF A TWO LAYER MODEL ATMOSPHERE

To explore the nature and validity of the approximations described in the previous chapter, a model two layer atmosphere with no winds is considered here. The fact that a two layer atmosphere is considerably simpler in computational features than a more realistic 30 layer atmosphere and that it exhibits most pertinent mathematical properties made such an exploratory study seem desirable.

3.1 Numerical Calculations in the Complex Plane

To investigate the appearance of a leaky mode, and hence an imaginary part to the complex horizontal wave number, a computer program that yields a pictorial display of the roots of the real and imaginary parts of the eigenmode dispersion function for particular values of ω was devised. A deck listing of this program appears in Appendix B. The printout from this program is arranged in two arrays. For any given ω, the arrays represent the sign (either + or -) of the real and imaginary parts of the eigenmode dispersion function. The abscissa and ordinate represent respectively the real and imaginary parts of the complex horizontal wave number. The real part of k is called AKR while the imaginary part is called AKI. By judiciously choosing the ranges for

the real and imaginary parts of the complex horizontal wave number and superimposing the two plots, a complex root should appear where the zeros of the real and imaginary parts of the normal mode dispersion function cross.

Figure 3 is the array plot computed by INFRASONIC WAVEFORMS for a two layer model atmosphere with no winds. The solid line depicts the third mode and traces its path to lower frequencies where it vanishes. By considering k to be complex and investigating the region where the mode vanishes a transition of the third mode to a leaky mode in this area should be verified. To pin down an area of ω in which to search for the leaky mode we consider G^2 for the upper halfspace which can be written as

$$G^2 = (\omega_{AU}^2-\omega^2)/c_U^2 + (\omega^2-\omega_{BU}^2)k^2/\omega^2 \qquad (3.1)$$

where

$$\omega_{AU} = \gamma g/2c_U \qquad (3.2)$$

and

$$\omega_{BU} = g(\gamma-1)^{1/2}/c_U \qquad (3.3)$$

where the subscript U designates the upper halfspace. When G^2 becomes negative and k complex we are presented with a

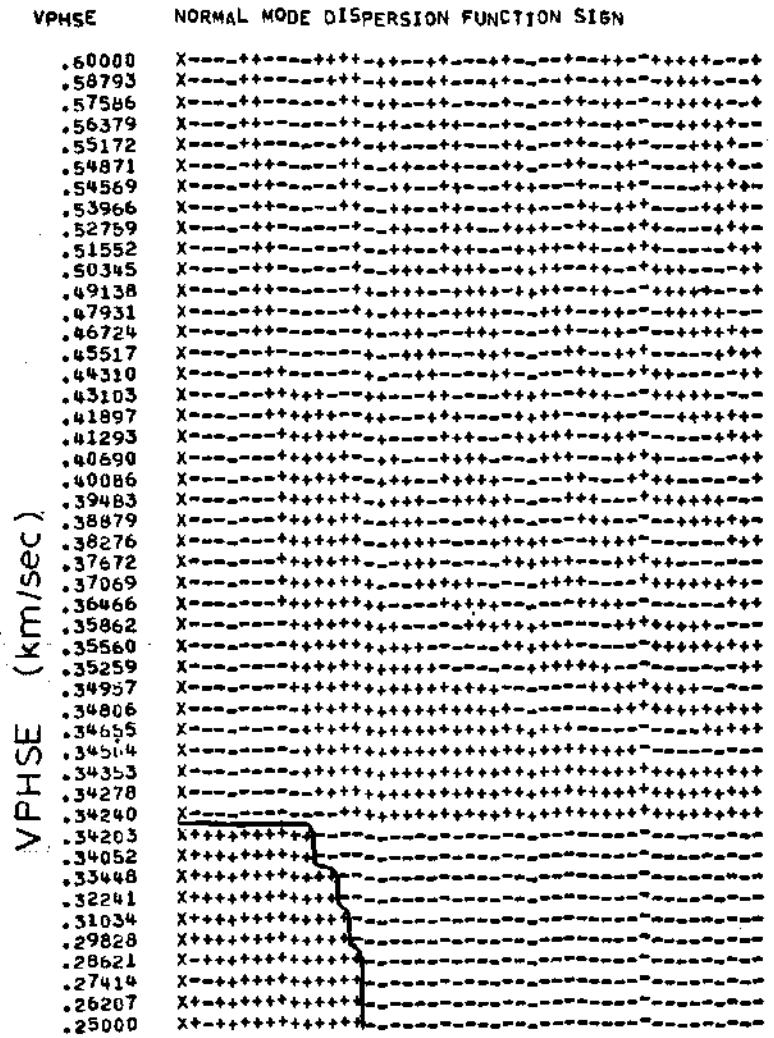

OMEGA =

.50000-02	.82759-02	.11552-01	.14828-01	.18103-01
.21379-01	.22198-01	.23017-01	.24655-01	.25065-01
.25269-01	.25372-01	.25474-01	.26293-01	.27931-01
.31207-01	.34483-01	.37759-01	.39397-01	.41034-01
.44310-01	.47586-01	.49224-01	.50862-01	.52500-01
.54138-01	.57414-01	.60690-01	.61509-01	.62328-01
.63966-01	.67241-01	.70517-01	.73793-01	.77069-01
.80345-01	.83621-01	.85259-01	.86897-01	.88534-01
.90172-01	.90991-01	.91810-01	.93448-01	.95086-01
.96724-01	.10000+00			

Angular Frequency (radians/sec)

Figure 3. Sign of the Eigenmode Dispersion Function for a Two Layer Atmosphere. Source is a 10 megaton explosion.

branch point at

$$k_B = \frac{\omega}{c} \left(\frac{\omega_{AU}^2 - \omega^2}{\omega_{BU}^2 - \omega^2}\right)^{1/2} \tag{3.4}$$

where the subscript B refers to the branch point. The corresponding phase velocity can be represented as

$$V_p = c_U \left(\frac{\omega^2 - \omega_{BU}^2}{\omega^2 - \omega_{AU}^2}\right)^{1/2} \tag{3.5}$$

From observing the value of the phase velocity where the third mode vanishes in Figure 2 (i.e., $V_p \approx .342$ km/sec) and using the value of the sound speed in the upper halfspace (i.e., $c_v = .8014$ km/sec) appearing in the same printout as Figure 2, we can approximate a search range in ω. Defining a parameter

$$r = V_p^2 / c_U^2 \tag{3.6}$$

and observing that $1-r^2$ is approximately equal to one in conjunction with noting that $\omega_{BU} + \omega \approx \omega$, Eq. (3.5) yields an equation of the form

$$\omega = \omega_{BU}(1-.1125\ r^2) \tag{3.7}$$

This equation describes a reasonable choice of a center point for a region in which to start the leaky mode search. A 20% margin is allowed on either side of ω. The margin on AKR is at least 30% on either side of the branch point for each value of ω. The range for AKI is partly determined by trial and error for which values yield the most descriptive plots and partly on the knowledge that the imaginary part of k is small for a leaky mode.[1]

The normal mode dispersion function is a multivalued function involving a branch cut for the case of a leaky mode and complex k. In investigating the appearance of complex roots using the computer program in Appendix B, a feel for the root history on the branches is desirable. To this end the normal mode dispersion function can be viewed as an equation of the form

$$F(\omega,k) + Q(\omega,k)[k_B-k^2]^{1/2} = 0 \qquad (3.8)$$

where k is a function of ω. Letting $k_o(\omega)$ be the root of $F(\omega,k_o) = 0$ then for k near k_o we have upon expanding

$$F = 0 + (\partial F/\partial k)_o(k-k_o) + \ldots = 0 \qquad (3.9)$$

and then the original dispersion relation is approximately

$$(\partial F/\partial k)_o(k-k_o) + Q(\omega,k_o)[k_B+k_o]^{1/2}[k_B-k_o]^{1/2} = 0 \qquad (3.10)$$

By letting

$$s = k-k_o \qquad (3.11a)$$

$$\epsilon = Q(\omega,k_o)[k_B+k_o]^{1/2}/(\partial F/\partial k)_o \qquad (3.11b)$$

$$s_p = k_B-k_o \qquad (3.11c)$$

and noting that k_B-k_o is small we obtain a prototype equation of the original cumbersome equation in the form of

$$s + \epsilon G = 0 \qquad (3.12)$$

where ϵ is small and may be either positive or negative. The quantity G is such that

$$G^2 = s_p-s \qquad (3.13)$$

The branch point is at $s = s_p$ and the branch cut moves to the right of s_p in the complex s plane. The phase of G is such that on the first branch G is real and positive along the real axis to the left of s_p. If the branch cut is chosen such that Re G>0 in the upper halfspace, Im G must have an

opposite sign to Im s and that Re $G \geq 0$ everywhere in the complex s plane. (See Fig. 4.)

If $s_p > 0$ then Eq. (3.12) has one real root which lies on the real axis to the left of s_p regardless of the sign of ε. This view is presented in Fig. 5. This real root can be represented by

$$s = -\varepsilon^2/2 - (\varepsilon^4/4+\varepsilon^2 s_p)^{1/2} \quad \text{for } \varepsilon > 0 \tag{3.14a}$$

$$s = -\varepsilon^2/2 + (\varepsilon^4/4+\varepsilon^2 s_p)^{1/2} \quad \text{for } \varepsilon < 0 \tag{3.14b}$$

For $\varepsilon > 0$ as s_p decreases from a finite value towards zero the root s is negative and moves to the right along the real axis towards $-\varepsilon^2$. Likewise for $\varepsilon < 0$ as s_p decreases from a finite value towards zero the root s is positive and moves to the left towards zero. When s_p passes through zero and becomes negative there are possibly two complex roots when $\varepsilon > 0$ and no roots when $\varepsilon < 0$. The $\varepsilon > 0$ result follows partly because Im s and Im G have opposite sign. There is a possibility of the imaginary part of Eq. (3.12) being zero when no such possibility exists for $\varepsilon < 0$ unless the root is purely real. So complex roots can at best only occur for the case $\varepsilon > 0$.

For $\varepsilon > 0$ there are two real roots for s when $0 > s_p > -\varepsilon^2/4$ these being

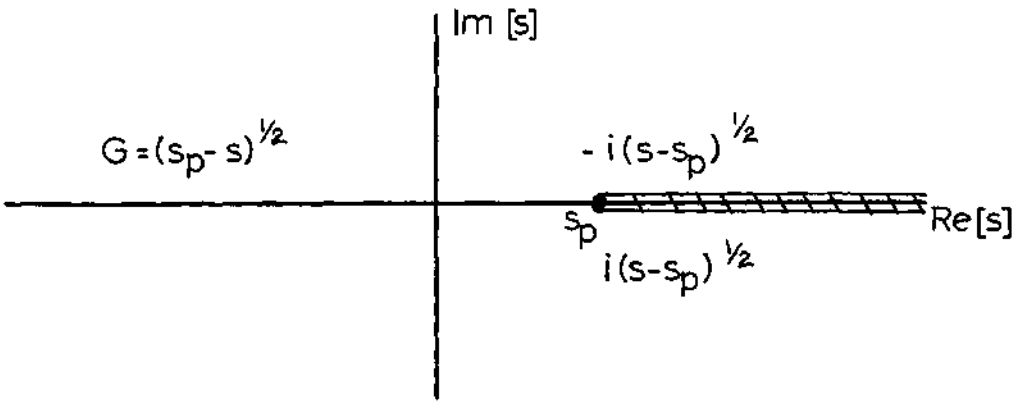

Figure 4. Complex s-Plane for Prototype Equation

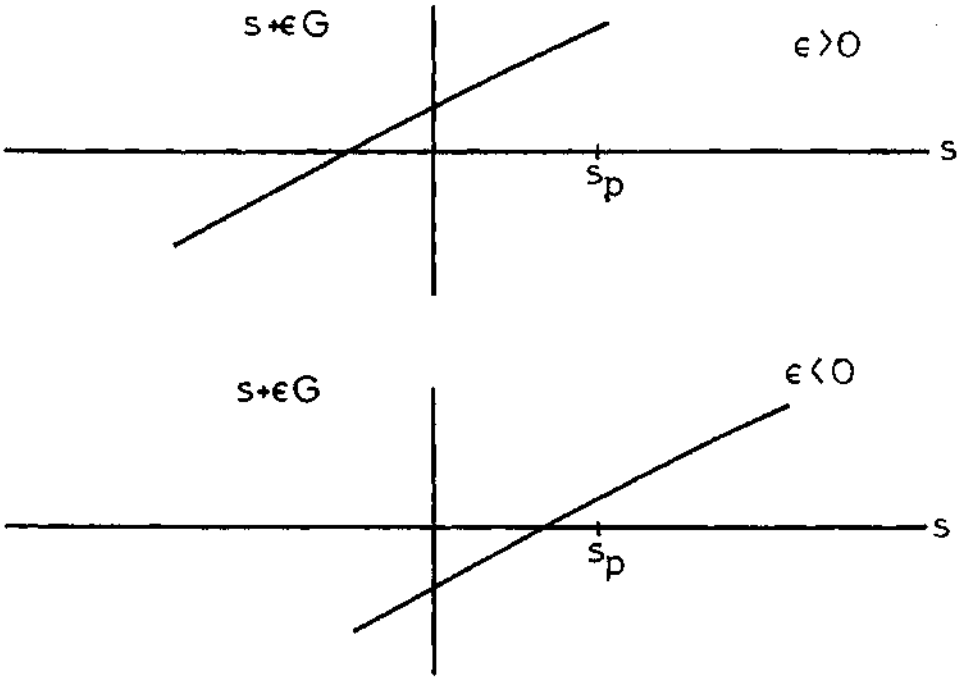

Figure 5. Illustration of Prototype Equation for $\varepsilon>0$ and $\varepsilon<0$

$$s = -\varepsilon^2/2 \pm (\varepsilon^4/4-\varepsilon^2|s_p|)^{1/2} \tag{3.15}$$

When $s_p = 0$, a second real root appears at $s = 0$ and this root moves to the left towards $-\varepsilon^2/2$ as s_p decreases further. The other root (- sign in Eq. (3.15)) is the continuation of the root which exists when $s_p>0$. Finally when $s_p<-\varepsilon^2/4$ the roots are complex and given by

$$s = -\varepsilon^2/2 \pm i(\varepsilon^2|s_p|-\varepsilon^4/4)^{1/2} \tag{3.16}$$

The general sequence of $\varepsilon>0$ is illustrated in Fig. 6. In summary, for $\varepsilon>0$, there is one root when $s_p>0$ but a second root is born at the branch point when $s_p = 0$. There are two separate real roots to the left of the branch point for a small range of negative s_p but these coalesce (still ahead of the branch cut) at $s = -\varepsilon^2/2$ when $s_p = -\varepsilon^2/4$. These two then split again and become complex as s_p moves further to the left.

There are no roots at all to the equation when $\varepsilon<0$ and $s_p<0$. For this case there are no complex roots as discussed previously. It follows that there are no real roots since s and εG are both negative to the left of s_p when $s_p<0$. This sequence is also illustrated in Fig. 6.

Modification of the preceding results to represent the eigenmode dispersion function as it is encountered in

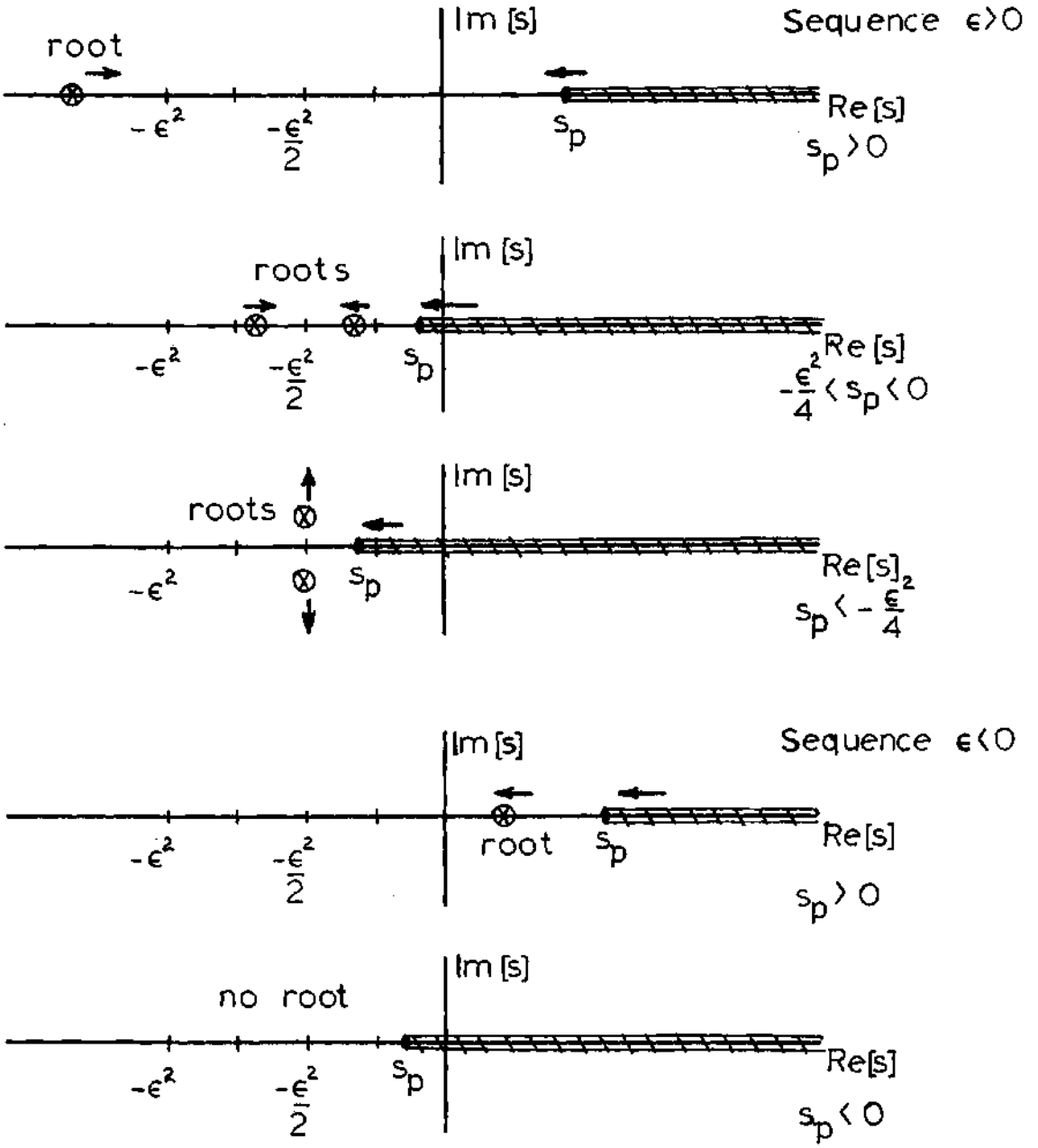

Figure 6. Root Sequence for $\varepsilon>0$ and $\varepsilon<0$

practice entails considering $\epsilon<1$ and $\epsilon<0$ for the case of complex k. Also, by using the conditions (1) s_p is assumed to have an arbitrarily small positive imaginary part; and (2) the branch line does not necessarily lie along the real axis and complex roots are sought where $s_I>0$ regardless of branch, the theory consistent with the above conditions developed by Pierce and Posey[1] yields explicit knowledge of the proper branch to search on for the roots of a leaky mode. As discussed before the two possible roots are represented by the equation

$$s = -\epsilon^2/2 \pm (\epsilon^4/4+\epsilon^2 s_p)^{1/2} \qquad (3.17a)$$

or equivalently

$$s = -\epsilon^2/2 \pm i(-\epsilon^4/4-\epsilon^2 s_p)^{1/2} \qquad (3.17b)$$

For real $s_p>-\epsilon^2/4$ only the root corresponding to the + sign in Eq. (3.17a) lies above the real axis when Im sp>0. For Re $s_p<-\epsilon^2/4$ one takes the + sign in Eq. (3.17b). Thus, in the limit Im $s_p \to 0$, the root of interest has the following behavior

$s_p>0$	$s>0$	I
$s_p = 0$	$s = 0$	

$$s_p = -\varepsilon^2/4 \qquad s = -\varepsilon^2/2 \qquad \text{II}$$

$$s_p < -\varepsilon^2/4 \qquad s = -\varepsilon^2/2 + i(\text{positive}) \qquad \text{II}$$

where Roman numerals refer to a branch. For $s_p > 0$ the root of interest lies on the first branch while $s_p < 0$ the root lies on the second branch. So complex roots do exist for leaky modes and $\varepsilon < 0$ but they occur on the second branch.

An extensive computer search for complex roots of the third and other modes was conducted using the computer program in Appendix B in a region of ω determined by Eq. (3.7). A typical printout for a particular value ω of the sign of the real and imaginary parts of the normal mode dispersion function for both branches appear in Figs. 7 through 10. A select amplification of the AKI scale for a mode other than the third is used to illustrate the complex roots appearing on the second branch. (See Figs. 11 and 12.) This figure also apparently shows the satisfaction of the Cauchy-Riemann conditions for an analytic eigenmode dispersion function. In all the cases examined for this model, no complex roots were found on either branch for the third mode. In this specific example then, the third mode can be said not to be leaking energy into the upper atmosphere. Figure 13 traces the root path (showing only the positive imaginary part of the root) for one of the other modes that were found to be leaking.

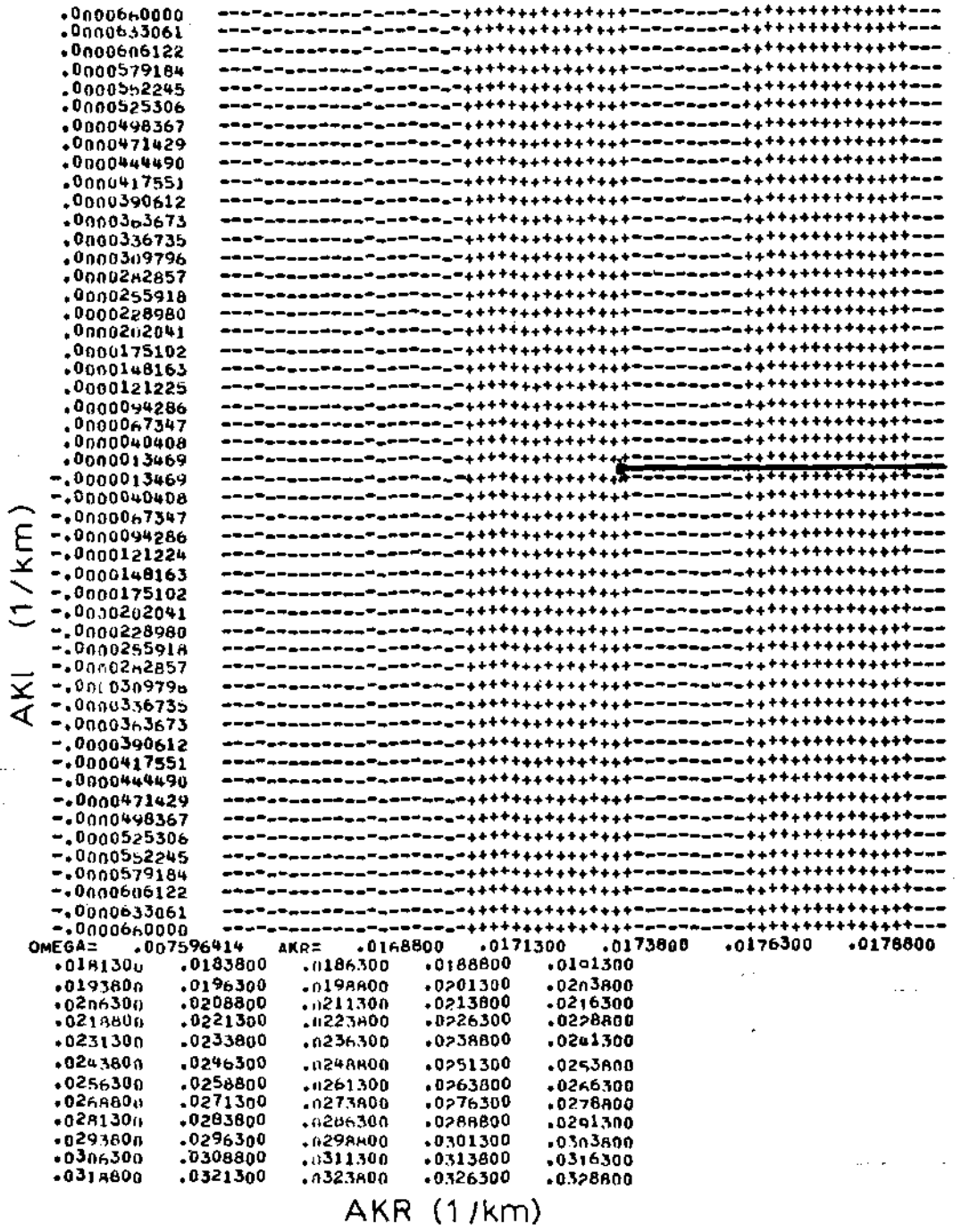

Figure 7. Sign of the Real Part of the Eigenmode Dispersion Function Showing Branch I

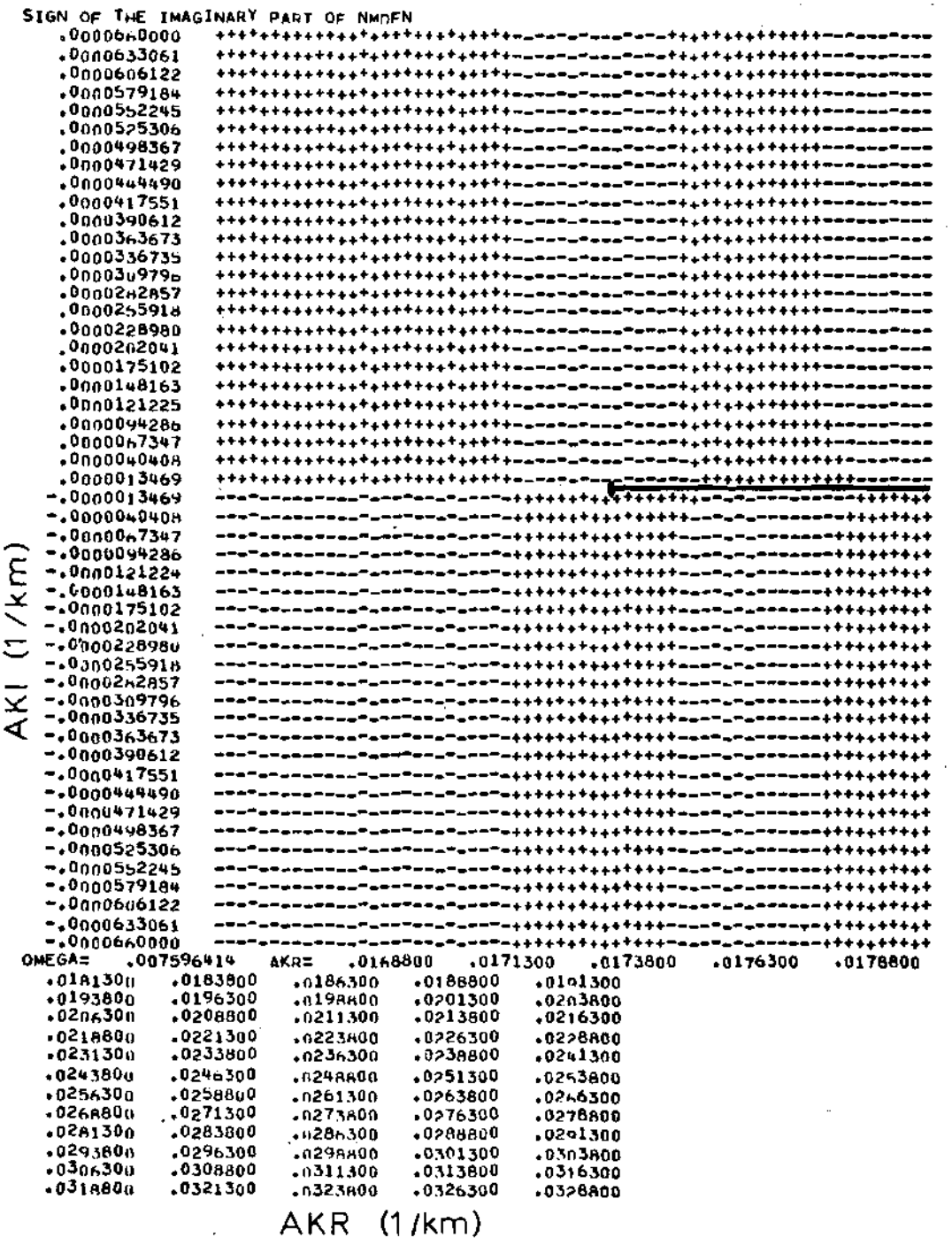

Figure 8. Sign of the Imaginary Part of the Eigenmode Dispersion Function Showing Branch I

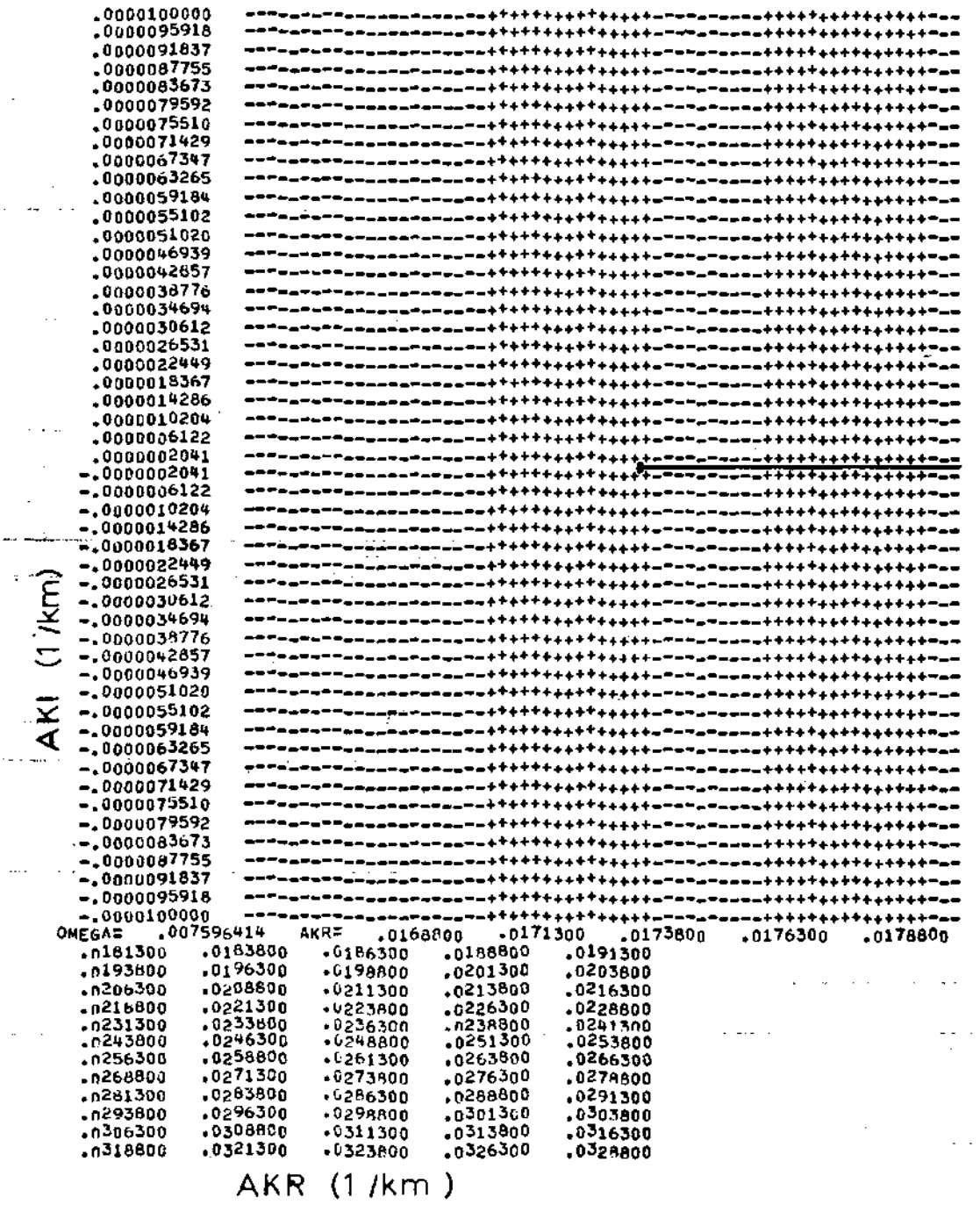

Figure 9. Sign of the Real Part of the Eigenmode Dispersion Function Showing Branch II

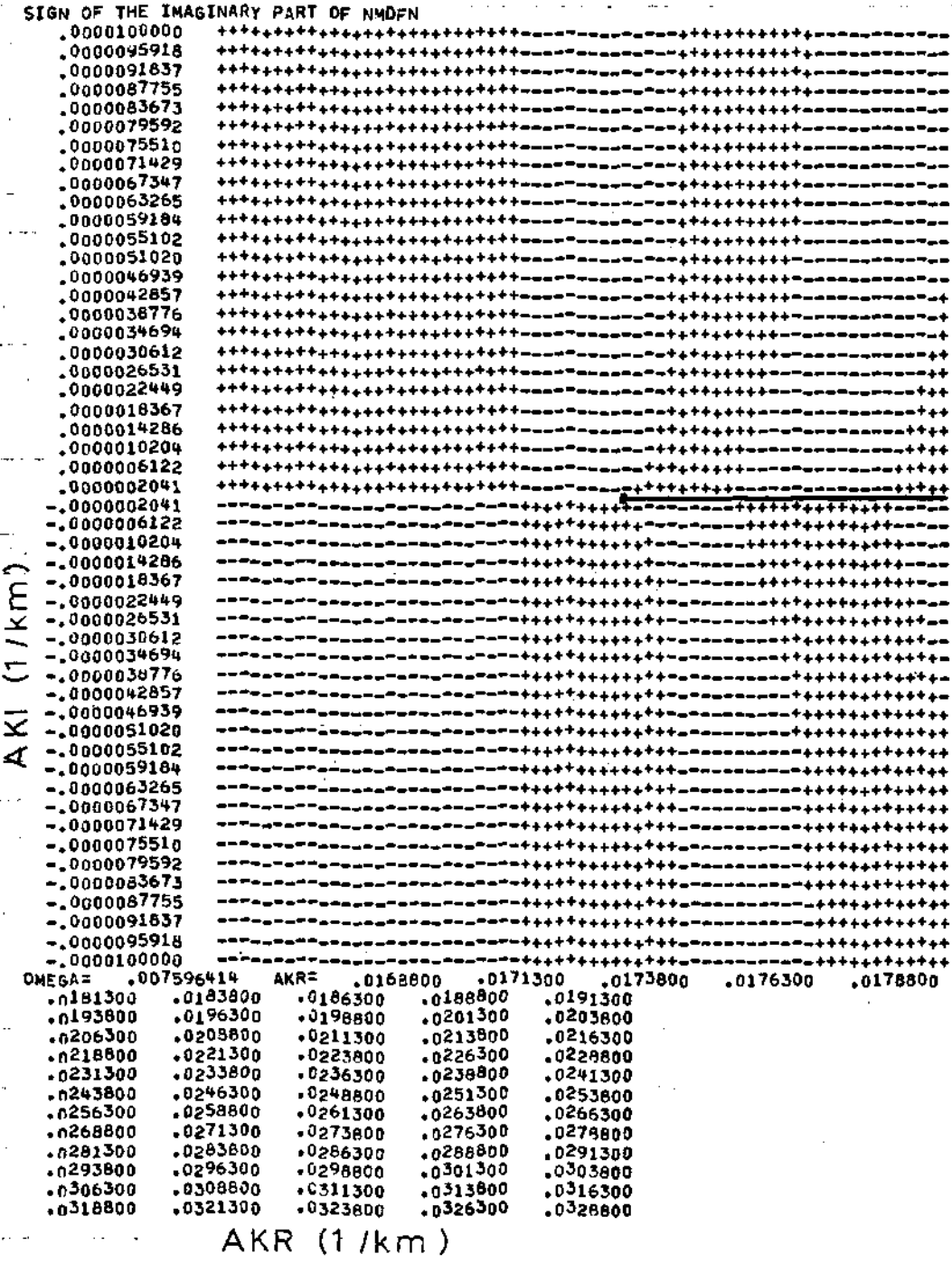

Figure 10. Sign of the Imaginary Part of the Eigenmode Dispersion Function Showing Branch II

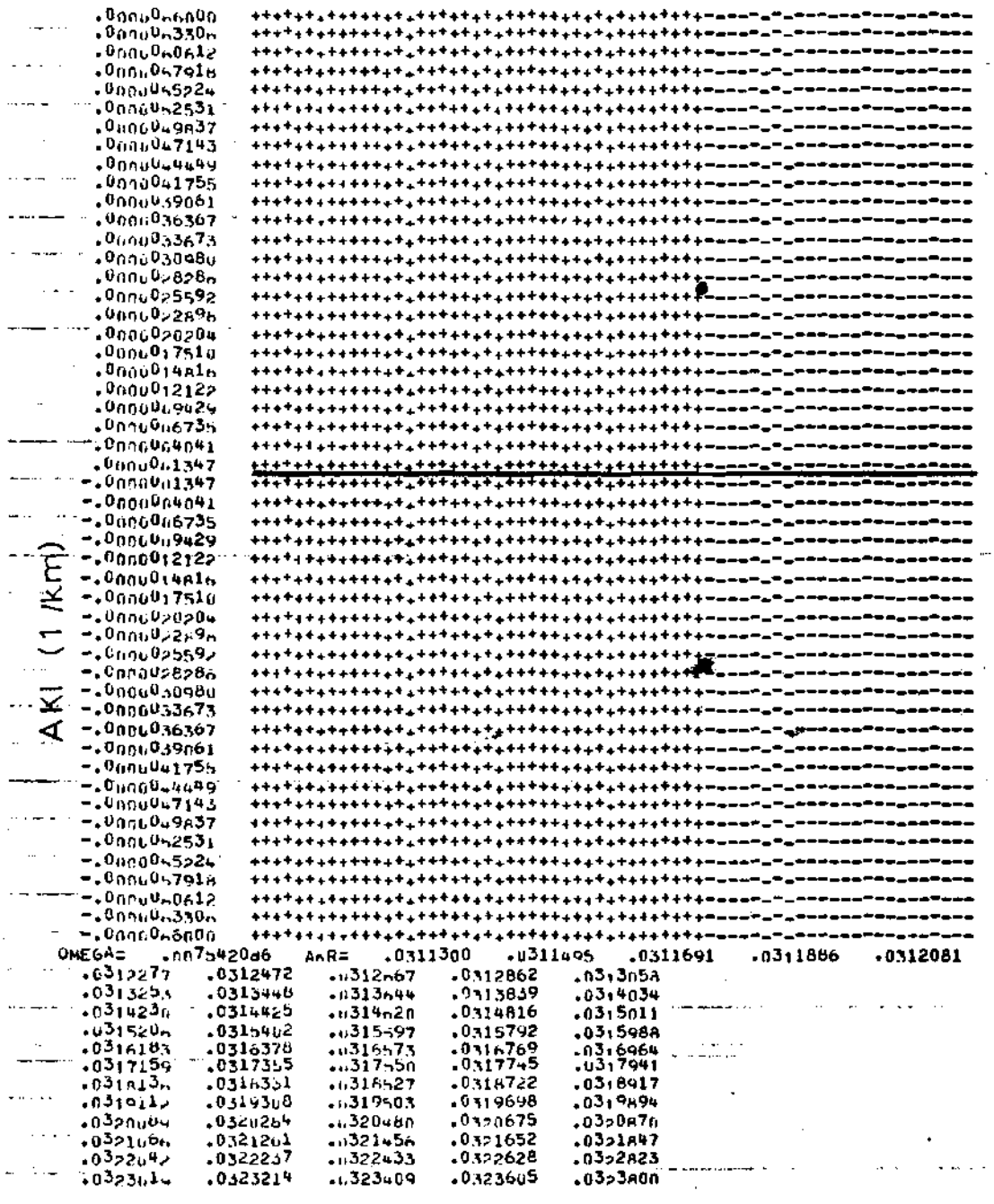

Figure 11. Sign of the Real Part of the Eigenmode Dispersion Function Showing Roots on Branch II

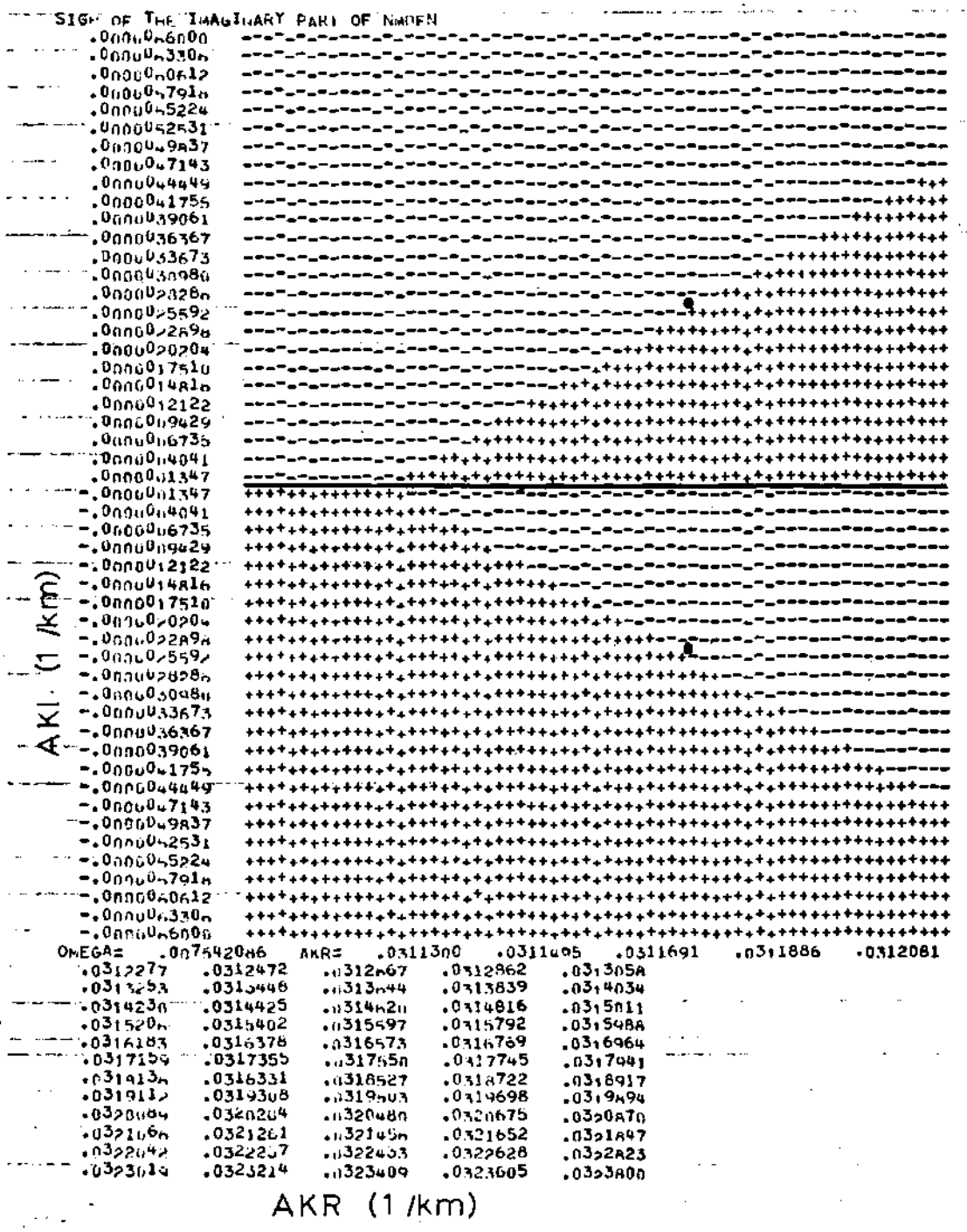

Figure 12. Sign of the Imaginary Part of the Eigenmode Dispersion Function Showing Roots on Branch II

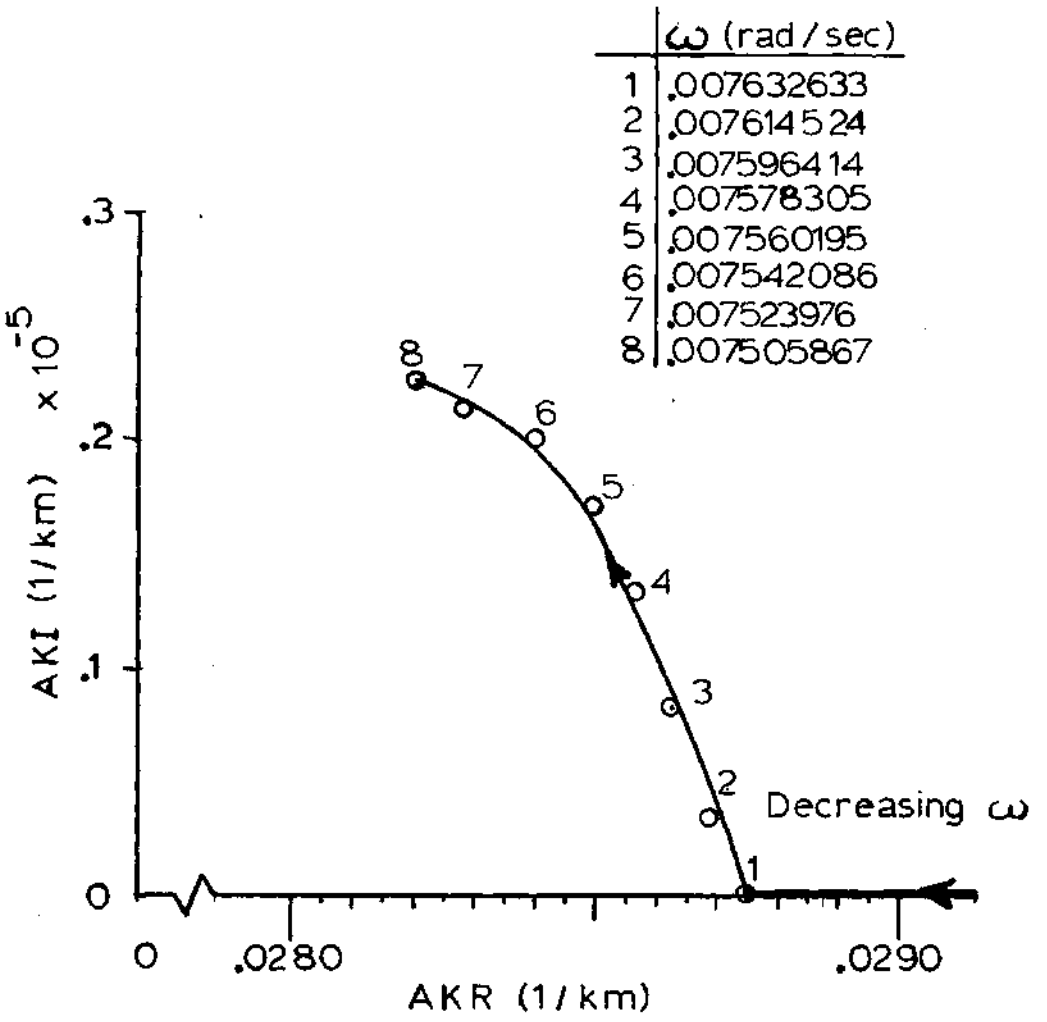

Figure 13. Positive Root Path for a Mode

3.2 Revised Theory for the Fundamental Mode

What is referred to as the third mode in the previous section is easily identified as the counterpart of Lamb's atmospheric edge mode for the isothermal atmosphere. As has been previously pointed out by Pierce and Posey,[2] this is the single most important mode for far field transmission of atmospheric infrasonic pressure waves in the one to ten minute period range. This mode is also referred to as the fundamental mode in the literature.

Since the fundamental mode corresponds to a wave dying off nearly exponentially with height above the ground, it should not be surprising that it is not much affected by the assumed nature of the upper atmosphere or that it should be leaky at low frequencies. However, it would seem to clarify mathematically why this is so within the context of the theoretical discussion given in the preceding section. In particular, one may note, that for this mode, the parameter ε in Eq. (3.12) is extremely small when k is set to k_o as in Eq. (3.11b). Thus in any event, one would expect $|\Delta k| = |s-s_o|$ to be extremely small. What is surprising in view of the analysis presented in the preceding section is that the imaginary part of k_I should be identically zero. To explain this, it is necessary to revise the approximation represented by Eq. (3.12) to

$$s + [\varepsilon_o + (\partial\varepsilon/\partial s)_o s]G = 0 \qquad (3.18)$$

where ε_o (previously termed simply ε) represents the value of ε at $k = k_o$ and $(\partial\varepsilon/\partial s)_o$ is the derivative of ε with respect to s evaluated at $s = 0$. From the above equation one has

$$s^2 = [\varepsilon_o + (\partial\varepsilon/\partial s)_o s]^2[s_p - s] \tag{3.19a}$$

or the cubic equation

$$D^2s^3 + (2D - D^2s_p + 1)s^2 + (\varepsilon_o^2 - 2Ds_p)s - \varepsilon_o^2 s_p = 0 \tag{3.20}$$

where, for brevity, we have abbreviated D for the derivative $(\partial\varepsilon/\partial s)_o$. One may note that this equation has at least one real root and moreover, all three roots will be real if (see for example, any edition of the Handbook of Chemistry and Physics).

$$b^2/4 + a^3/27 \leq 0 \tag{3.21}$$

where

$$a = [3D^2(\varepsilon_o^2 - 2Ds_p) - (2D - D^2s_p + 1)^2]/3D^4 \tag{3.22a}$$

$$b = [2(2D - D^2s_p + 1)^3 - 9D^2(\varepsilon_o^2 - Ds_p)(2D - D^2s_p + 1) - 27D^4\varepsilon_o^2 s_p]/27D^6 \tag{3.22b}$$

In order for (3.21) to be satisfied, one must at least have $a<0$ and this will be true if

$$\varepsilon_o^2 < (2D-D^2 s_p+1)^2/3D^2+2Ds_p$$

which would certainly be the case were the magnitude of D sufficiently large. It is also noted that in the limit of large D

$$a \to -s_p^2/3 - (2/3)(s_p/D)$$

$$b \to -(2/27)s_p^3 - (21/27)s_p^2/D$$

and (3.21) would imply

$$b^2/4 + a^3/27 \to 5\, s_p^5/(a)(27)D$$

So there would be three real roots in this limit as long as $s_p<0$. However, it is precisely when $s_p<0$ that one would look for a complex root. Thus it is expected that, if D is sufficiently large and ε_o sufficiently small, one would find no complex roots.

Insofar as the computational method described in Chapter II is concerned, the modification of it to incorporate what would correspond to the term $(\partial\varepsilon/\partial s)_o s$ in Eq. (3.19) (such that Eq. (2.28) would be altered correspondingly) has

not yet been carried out. While this is not a very difficult task, it would seem of low priority insofar as the actual correction to k_o would be extremely small in those cases where the actual correction differed in relative value from that predicted by using Eq. (2.28).

CHAPTER IV

EXTENSION OF INFRASONIC WAVEFORMS TO INCLUDE DISTANCES BEYOND THE ANTIPODE

Previous theoretical considerations incorporated into the digital computer program INFRASONIC WAVEFORMS restricted synthesis to waves that had traveled less than one-half the distance around the earth. The purpose of this chapter is to further exemplify techniques to enable computer synthesis of acoustic-gravity pressure waveforms at points whose distances are greater than halfway around the world from a nuclear explosion. Extension of prior theory shows that for wave propagation past a point on a spherical earth, one-half the great circle distance away from the point of detonation (i.e., the antipode), a phase shift of $\pi/2$ radians to the Fourier transforms of each modal wave is incurred. Modification to the computer program necessitates the reinterpretation of the great circle distance r, the inclusion of the $\pi/2$ phase shift, and a modification to the earth curvature correction factor. Computations are presented for pre and post antipodal waveforms.

4.1 Theoretical Considerations for Post Antipodal Waveforms

In considering acoustic-gravity waves that have passed

beyond the antipode, certain specific definitions for the various waveforms must be adopted. To an observer located on the surface of a spherical earth between the source and the antipode the pressure waveform that is first observed is the direct arrival or A_1 arrival. The A_1 arrival has traveled the shortest great circle distance r to reach the observation point. The next waveform observed at the above observation point is the A_2 or antipodal arrival. The A_2 arrival has traveled the longer great circle distance from the explosion point around the globe passing through the antipode to reach the observation point. The A_3 arrival is the A_1 pressure waveform that has traveled completely around the globe with respect to the observation point having passed through the observation point, the antipode, the detonation point, and back to the observation point. Further arrivals exist but are not considered here. The distance r is measured in kilometers and is the great circle distance measured from the detonation point to the final observation point. Figure 14 shows some typical pressure waveforms recorded in suburban New York for the Russian explosion of 58 megatons at Novaya Zemlya on 30 October 1961.[5]

Previous numerical syntheses of acoustic-gravity waveforms have only considered direct arrivals. The extension of this theory to include waveform prediction for antipodal arrivals is described here. An investigation of a small region of the earth's surface in the vicinity of the antipode

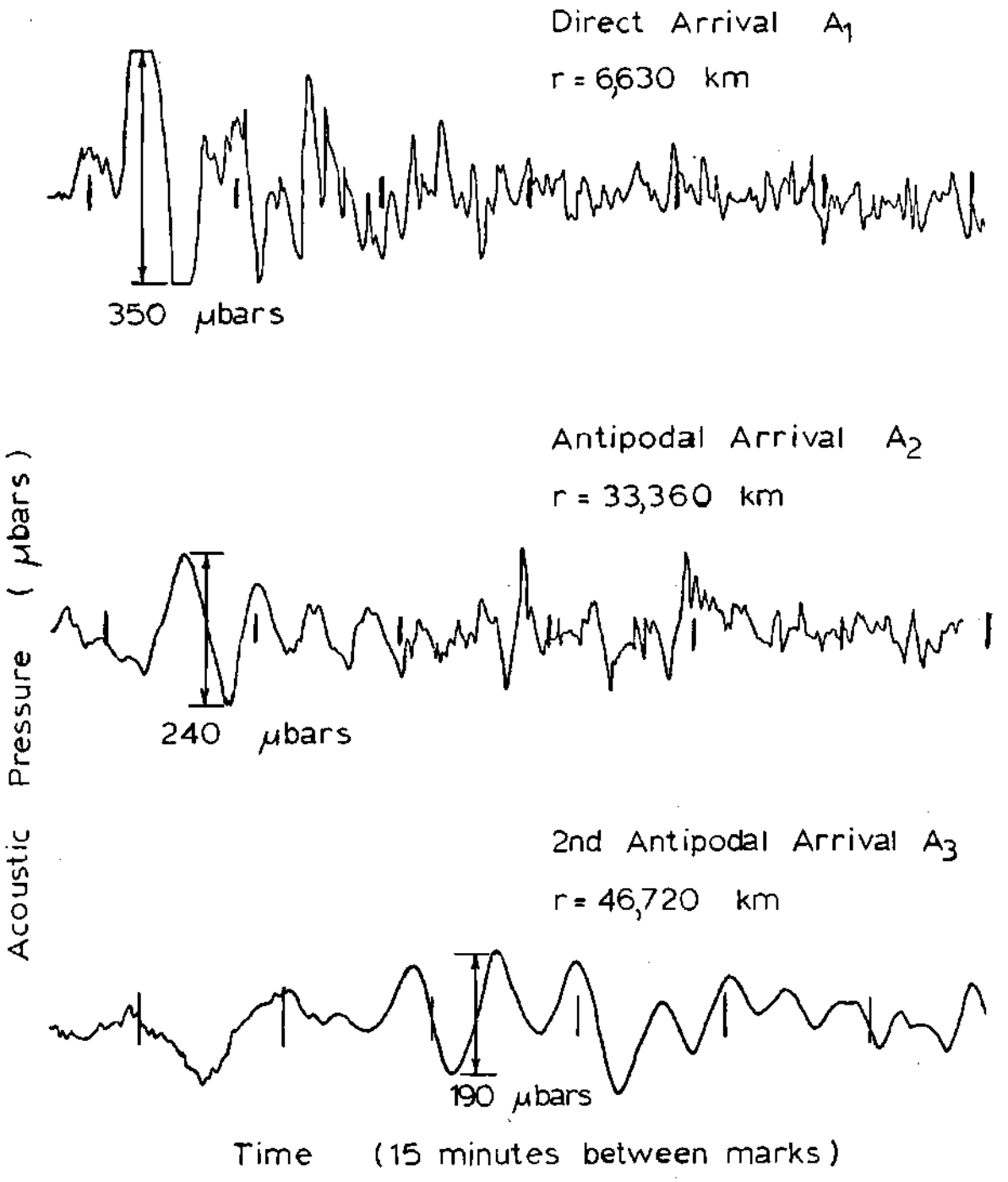

Figure 14. Typical Pressure Waveforms.[5] Recorded in suburban New York for 58 megaton Soviet test at Novaya Zemlya on 30 October 1961.

where prior theory breaks down yields certain waveform characteristics that enable waveform synthesis to be extended to ranges past the antipode. By taking the antipodal region smaller in area than say 1/100th of the earth's area as a whole we can consider this region to be flat. Then the equation governing propagation of any frequency in any guided mode near the antipode is the cylindrical wave equation in the form of

$$\partial^2 F/\partial r_A^2 + (1/r_A)\partial F/\partial r_A - (1/V_p^2)\partial^2 F/\partial t^2 = 0 \qquad (4.1)$$

where F would represent the r_A and t dependent part of the integration kernal for synthesization. (i.e., Integration over frequency of any given modal waveform where the height dependent part is omitted here.) The quantity V_p is the corresponding phase velocity. The assumed circular symmetry of the wave about the antipode is inherent in the absence of the angular derivative terms in the above equation. The distance r_A is measured positive out from the antipode. The wave solution to Eq. (4.1) for the total acoustic pressure p and small r_A can be written for time t as

$$F \approx DJ_o(kr_A)\cos(\omega t+\varepsilon) \qquad (4.2)$$

For the above, $k = \omega/V_p$ represents the horizontal wave number, ω the angular frequency, and ε some phase angle.

The quantity D is some arbitrary constant while $J_o(kr_A)$ is the Bessel function of zero order.

When r_A is sufficiently large (i.e., greater than three wavelengths) a solution for the total acoustic pressure p can be considered as a sum of ingoing and outgoing waves with respect to the antipodal region. The asymptotic solution for large kr_A can be written for time t as

$$F \approx A(r_A)^{-1/2}\cos(\omega t+kr_A+\phi_{in}) \qquad (4.3)$$

$$+ B(r_A)^{-1/2}\cos)\omega t-kr_A+\phi_{out})$$

In Eq. (4.3) ϕ is some phase angle while ω and k are as previously defined. The minus sign in the argument of the cosine denotes an ingoing wave. Equation (4.3) is not defined at $r_A = 0$ and as r_A approaches zero, wave amplification is predicted. Figure 15 illustrates waveform amplification approaching the antipode for three different values of r for a ten megaton nuclear explosion. The antipode is reached when $r \approx 20{,}000$ km.

Realizing that Eqs. (4.2) and (4.3) should represent the same pressure waveform at large r_A we can now show the existence of a phase difference between waveforms approaching and leaving the antipode. For large r_A, the Bessel function $J_o(kr_A)$ can be represented by its asymptotic approximation such that Eq. (4.2) becomes

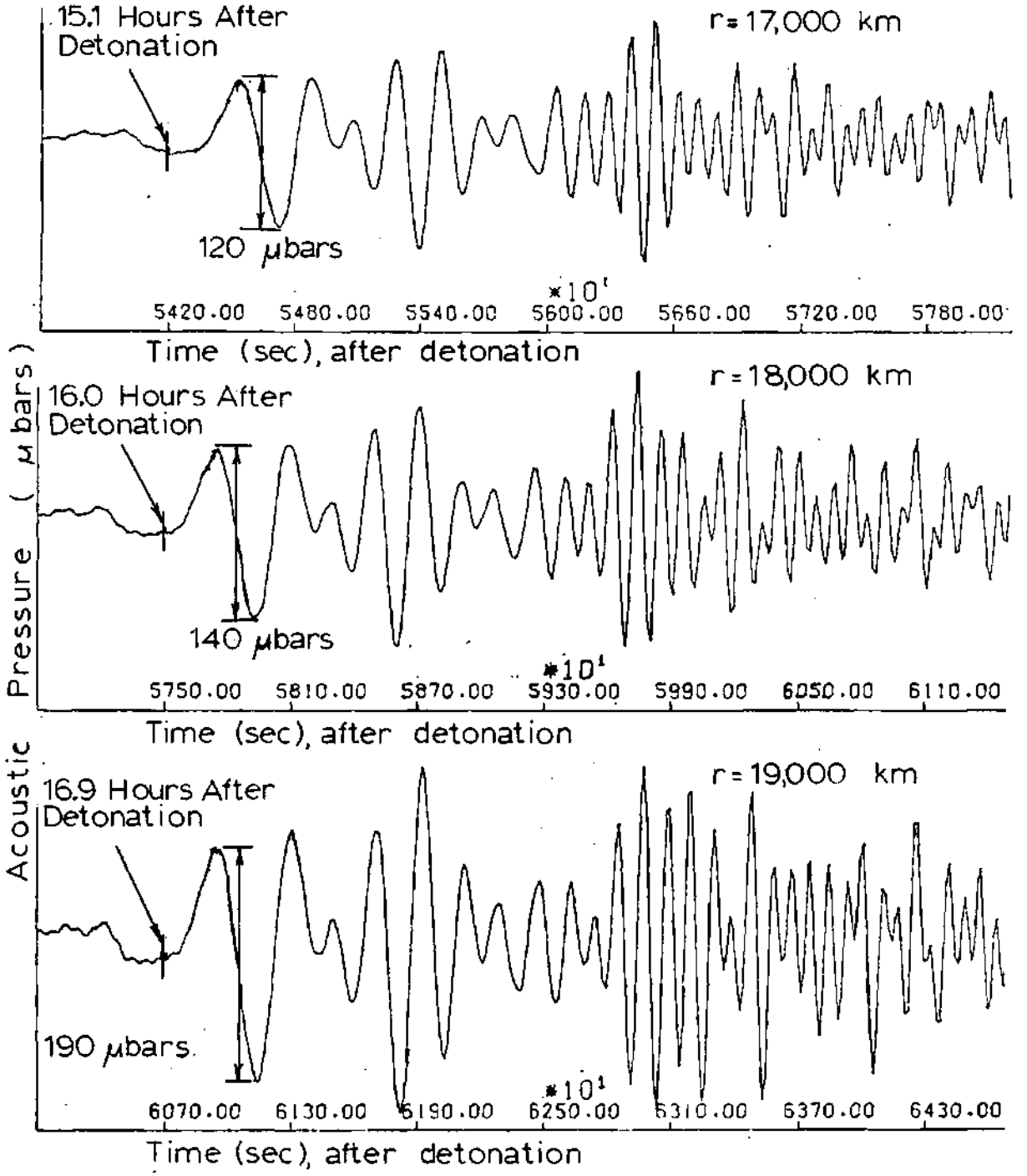

Figure 15. Synthesized Waveform Amplification Before the Antipode. Source is a 10 megaton explosion.

$$F \approx D(2/\pi r_A k)^{1/2} \cos(kr_A - \pi/4)\cos(\omega t + \varepsilon) \tag{4.4}$$

or with the aid of trigonometric identities as

$$F \approx \frac{1}{2} D(2/\pi r_A k)^{1/2} [\cos(\omega t + \varepsilon + kr_A - \pi/4) + \cos(\omega t + \varepsilon - kr_A + \pi/4)] \tag{4.5}$$

Equating (4.3) to (4.5) then requires that

$$A = B = D/(2\pi k)^{1/2} \tag{4.6a}$$

$$\phi_{in} = \varepsilon - \pi/4 \tag{4.6b}$$

$$\phi_{out} = \varepsilon + \pi/4 \tag{4.6c}$$

so

$$\phi_{out} = \phi_{in} + \pi/2 \tag{4.7}$$

The latter shows that a pressure waveform undergoes a phase shift of 90 degrees. Based on this knowledge the computer program has been altered to synthesize pressure waveforms for the A_2 arrival that passes through the antipode.

4.2 Modifications to INFRASONIC WAVEFORMS for Post Antipodal Waveforms

Waveform synthesis for ranges beyond the antipode necessitates only minor adjustments to the computer program. By considering the theoretical development of Brune, Nafe, and Alsop (1961)[6] for circular spreading of waves over a spherical surface of radius r_e (i.e., r_e = 6374 km for earth) the amplitude correction factor for the curvature of a spherical earth, appearing in subroutine TMPT, is altered for post antipodal waveforms by replacing the term $\sin(r/r_e)$ by its absolute magnitude. Where r is interpreted as the total distance the wave has traveled from the point of detonation. For post antipodal arrivals considered here r would be between πr_e and $2\pi r_e$ kilometers. The earth curvature correction factor in subroutine TMPT appearing as

```
CF = (1./(6374. * SIN(RAD)))**0.5          (4.8)
```

is replaced for post antipodal waveforms by

```
CF = (1./(6374.*ABS(SIN(RAD))))**0.5       (4.9)
```

where ROBS = r and

```
RAD = ROBS/6374.                           (4.10)
```

To accommodate the change in phase as the waveforms pass through the antipode two computer cards of the form

$$PH2 = PH2 + 1.570796 \qquad (4.11)$$

are inserted in the deck listing of subroutine TMPT after lines 160 and 177.

After incorporating the above modifications into subroutine TMPT the computer program was then utilized to synthesize various theoretical waveforms. Using the Soviet shot of 30 October 1961 as the source, a phase shift upon passing through the antipode is exhibited in Fig. 16 for two observation ranges of a synthesized pressure waveform. Further dispersion beyond the antipode of the pressure waveform is shown in Fig. 17 for a ten megaton explosion. A comparison of antipodal arrivals for a computer synthesized pressure waveform and a microbarograph recorded by Donn and Shaw in suburban New York[5] for the 58 megaton Soviet test is presented in Fig. 18. Considering the scattering in waveforms that can occur at such large arrival distances, it is not unreasonable to say that the amplitudes and typical periods of the two plots are of the same order of magnitude.

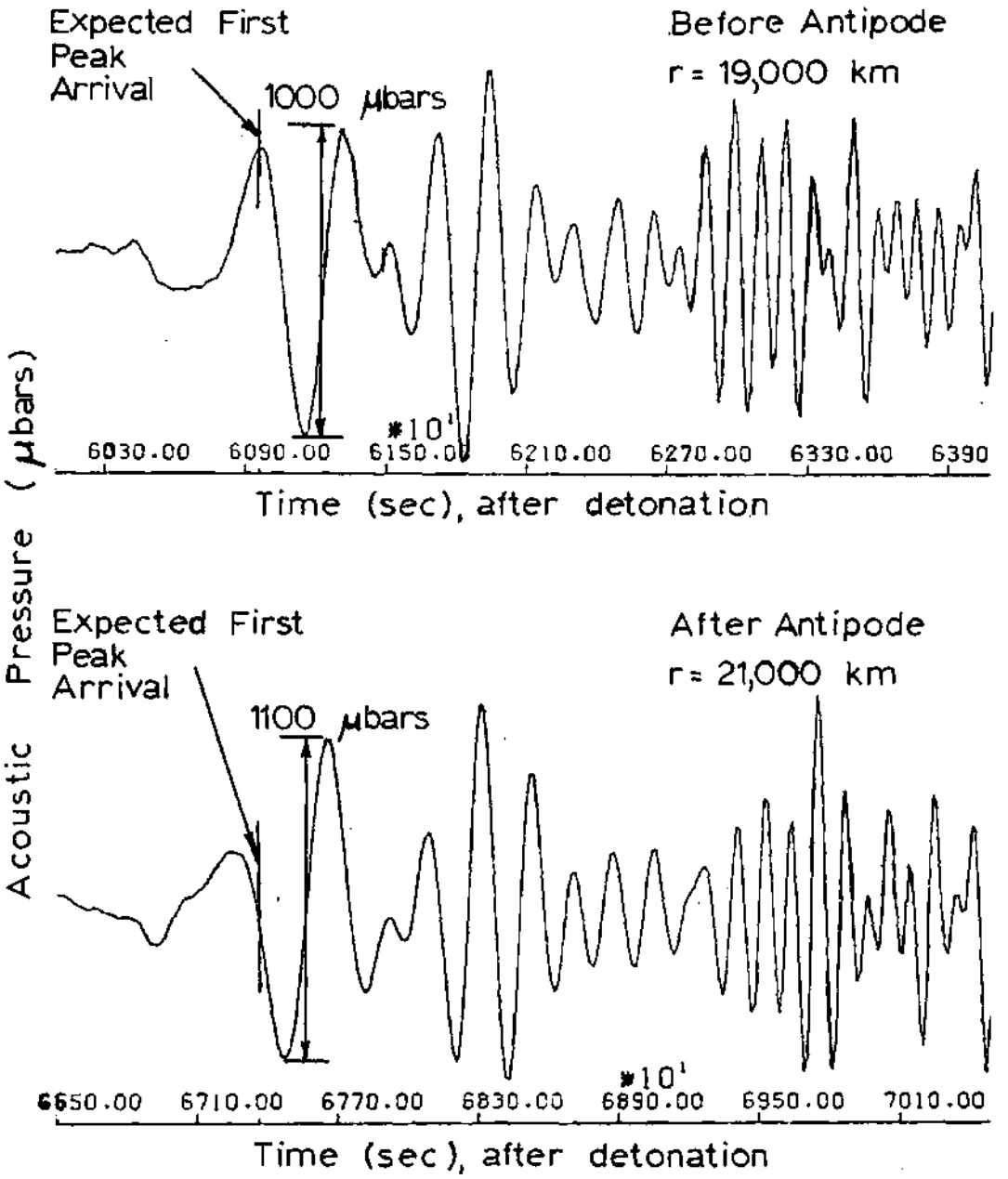

Figure 16. Phase Shift on Passing Through Antipode for a Synthesized Waveform. Source is 58 megaton Soviet test at Novaya Zemlya.

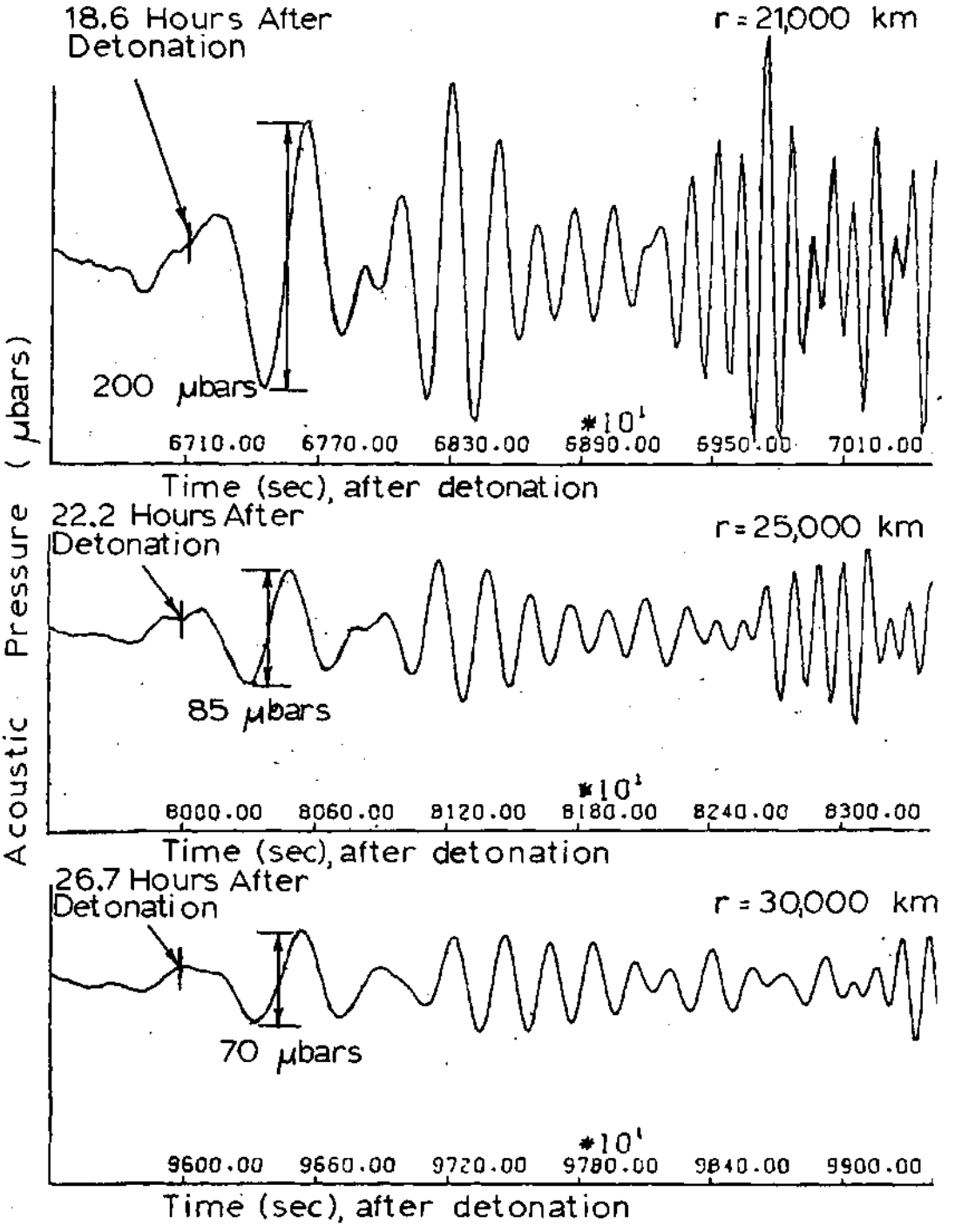

Figure 17. Synthesized Waveform Dispersion Beyond the Antipode. Source is a 10 megaton explosion.

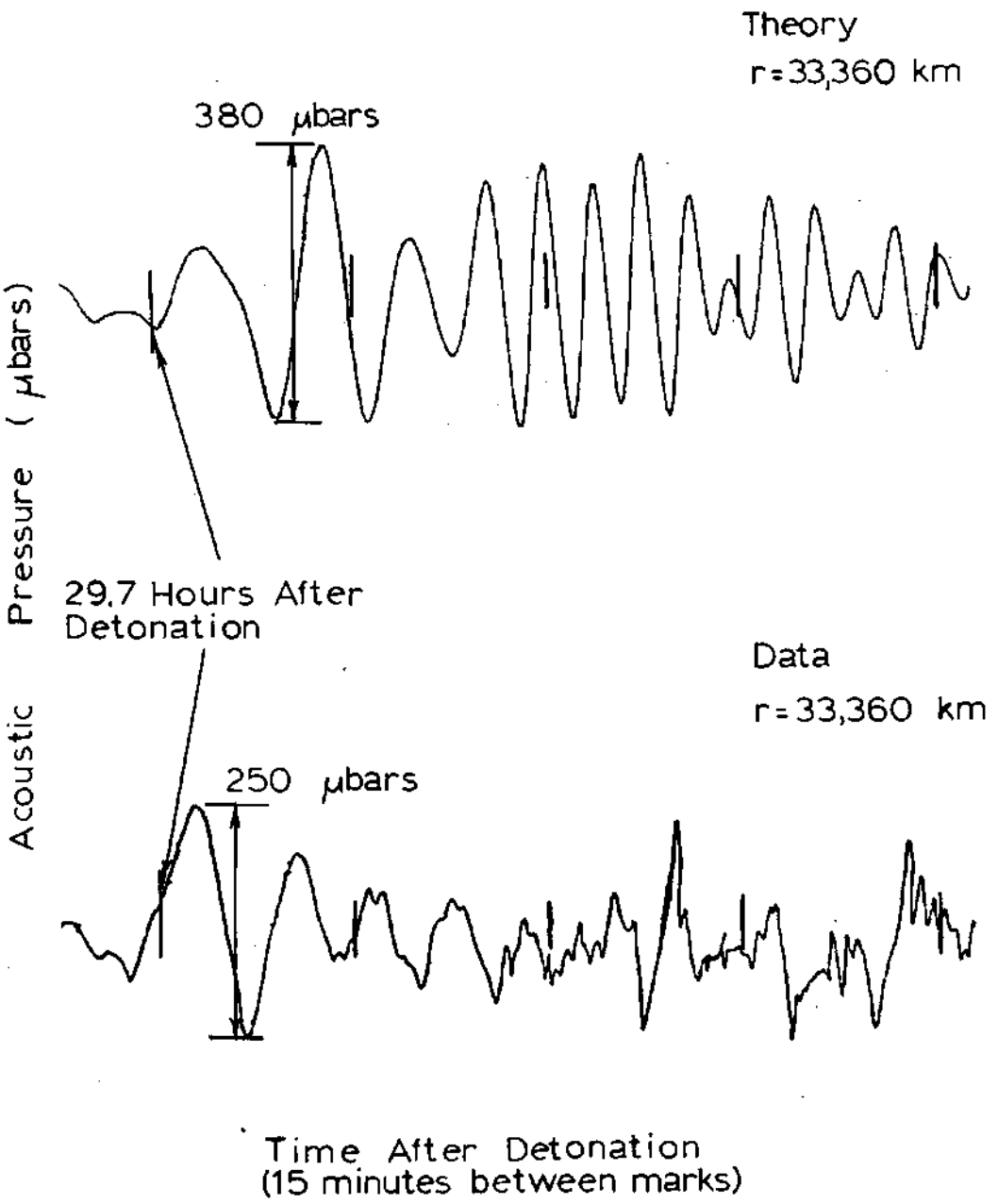

Figure 18. Theory and Data for Antipodal Arrivals. Source is 58 megaton Soviet test at Novaya Zemlya. Data recorded in suburban New York by W. L. Donn and colleagues. Amplitude scales are not matched.

CHAPTER V

CONCLUSIONS AND RECOMMENDATIONS

On the basis of the preceding chapters certain conclusions can be drawn as to the extension of the digital computer program INFRASONIC WAVEFORMS to include antipodal waveforms and leaky modes.

By altering only a few cards in subroutine TMPT antipodal waveforms can be accommodated. The principal modification was a 90 degree phase shift for waves passing through the antipode.

The investigation for the inclusion of weakly leaking modes determined that the normal mode dispersion function can be extended into leaky mode regions. The search in a two layer atmosphere for the imaginary part of the complex horizontal wave number that is inherent in such leaky modes showed a non-leaky third mode with the complex roots for other modes appearing on the second branch.

Furthermore, a comprehensive technique for incorporating leaky modes in actual waveform synthesis for realistic model atmospheres has been outlined. It is anticipated that the detailed implementation of this technique will be carried out in the very near future.

APPENDICES

APPENDIX A

SUBROUTINES DADQR, DMDQR, AND DRDQR

This Appendix contains the deck listings of subroutines DADQR, DMDQR, and DRDQR. The listings also include a short introduction and a description of the input and output parameters for each subroutine.

```
C     DADQR  (SUBROUTINE)  MODIFIED 7/11/74  LAST CARD IN DECK IS NO.
C
C
C                    ----ABSTRACT----
C
C TITLE - DADQR
C         THE FUNCTION OF THIS SUBROUTINE IS TO COMPUTE THE COMPONENTS
C         OF THE MATRICES DADOM,DADKX, AND DADKY WHICH REPRESENT THE
C         PARTIAL DERIVATIVES OF THE MATRIX A WHICH WOULD BE
C         COMPUTED BY SUBROUTINE AAAA.
C              DADOM IS THE PARTIAL DERIVATIVE MATRIX OF A WRT OMEGA
C              DADKX IS THE PARTIAL DERIVATIVE MATRIX OF A WRT AKX
C              DADKY IS THE PARTIAL DERIVATIVE MATRIX OF A WRT AKY
C         LIKE A, ALL ARE 2-BY-2 MATRICES.
C
C LANGUAGE - FORTRAN V (UNIVAC 1108,REFERENCE MANUAL UP-7536 REV. 1)
C AUTHORS - ALLAN D. PIERCE, CHRISTOPHER KAPPER, G.I.T., JULY, 1974
C
C                    ----CALLING SEQUENCE----
C
C SEE SUBROUTINE COMPK
C     DIMENSION D(2,2),DADOM(2,2),DADKX(2,2),DADKY(2,2)
C     CALL DADQR(OMEGA,AKX,AKY,C,VX,VY,DADOM,DADKX,DADKY)
C
C NO EXTERNAL SUBROUTINES REQUIRED
C
C                    ----ARGUMENT LIST----
C
C
C     OMEGA       R*4     NO      INP
C     AKX         R*4     NO      INP
C     AKY         R*4     NO      INP
C     C           R*4     NO      INP
C     VX          R*4     NO      INP
C     VY          R*4     NO      INP
C     DADOM       R*4     2-BY-2  OUT
C     DADKX       R*4     2-BY-2  OUT
C     DADKY       R*4     2-BY-2  OUT
C
C NO COMMON STORAGE USED
C
C                    ----INPUTS----
C
C
C     OMEGA       =ANGULAR FREQUENCY  RAD/SEC
C     AKX         =X COMPONENT OF HORIZONTAL WAVE NUMBER VECTOR IN 1/KM
C     AKY         =Y COMPONENT OF HORIZONTAL WAVE NUMBER VECTOR IN 1/KM
C     C           =SOUND SPEED IN KM/SEC
C     VX          =X COMPONENT OF WIND VELOCITY IN KM/SEC
C     VY          =Y COMPONENT OF WIND VELOCITY IN KM/SEC
C
C                    ----OUTPUTS----
C
C
C     DADOM(I,J)  =(I,J)-TH ELEMENT OF DADOM MATRIX
C     DADKX(I,J)  =(I,J)-TH ELEMENT OF DADKX MATRIX
C     DADKY(I,JE  =(I,J)-TH ELEMENT OF DADKY MATRIX
C
C                    ----PROGRAM FOLLOWS BELOW----
C
      SUBROUTINE DADQR(OMEGA,AKX,AKY,C,VX,VY,DADOM,DADKX,DADKY)
C     DADOM,DADKX,DADKY ARE MATRIX DERIVATIVES OF A WITH RESPECT TO
C     OMEGA,AKX,AKY, WHERE A IS AS COMPUTED BY AAAA.
      DIMENSION D(2,2),DADOM(2,2),DADKX(2,2),DADKY(2,2)
      CSQ=C*C
```

```
63*           D(1,1)=.0098
64*           D(1,2)=-CSQ
65*           D(2,1)=(96.04E-6)/CSQ
66*           D(2,2)=-.0098
67*           BOM=OMEGA-AKX*VX-AKY*VY
68*           BOMSQ=BOM**2
69*     C     T IS AKSQ/BOMSQ
70*           DTDOM=-2.0*(AKX**2+AKY**2)/(BOMSQ*BOM)
71*           DTDKX=-DTDOM*VX+2.0*AKX/BOMSQ
72*           DTDKY=-DTDOM*VY+2.0*AKY/BOMSQ
73*           DO 90 I=1,2
74*           DO 90 J=1,2
75*           DADOM(I,J)=DTDOM*D(I,J)
76*           DADKX(I,J)=DTDKX*D(I,J)
77*        90 DADKY(I,J)=DTDKY*D(I,J)
78*     C     THE ABOVE ELEMENTS ARE CORRECT EXCEPT FOR (2,1) ELEMENTS
79*           XAT=2.0*BOM/CSQ
80*     C     XAT IS THE DERIVATIVE WITH RESPECT TO OMEGA OF BOMSQ/CSQ
81*           DADOM(2,1)=DADOM(2,1)-XAT
82*           DADKX(2,1)=DADKX(2,1)+XAT*VX
83*           DADKY(2,1)=DADKY(2,1)+XAT*VY
84*           RETURN
85*           END
```

```
C     DMDDR  (SUBROUTINE)  MODIFIED  7/11/74  LAST CARD IN DECK IS NO.
C
C                         ----ABSTRACT----
C
C TITLE - DMDDR
C         THE FUNCTION OF THIS SUBROUTINE IS TO COMPUTE THE COMPONENTS
C         OF THE MATRICES DMDDM,DMDKX, AND DMDKY WHICH REPRESENT THE
C         PARTIAL DERIVATIVES OF THE EM MATRIX WHICH WOULD BE
C         COMPUTED BY SUBROUTINE MMMM.
C              DMDDM IS THE PARTIAL DERIVATIVE MATRIX OF EM WRT OMEGA
C              DMDKX IS THE PARTIAL DERIVATIVE MATRIX OF EM WRT AKX
C              DMDKY IS THE PARTIAL DERIVATIVE MATRIX OF EM WRT AKY
C         MATRIX EM IS ALSO COMPUTED IN THIS SUBROUTINE.
C
C LANGUAGE - FORTRAN V (UNIVAC 1108,REFERENCE MANUAL UP-7536 REV.1)
C
C AUTHORS - ALLAN D PIERCE,CHRISTOPHER KAPPER, G.I.T., JULY, 1974
C
C                 -- -- ----CALLING SEQUENCE----
C
C SEE SUBROUTINE COMPK
C     DIMENSION A(2,2),EM(2,2),DMDX(2,2)DMDDM(2,2),DMDKX(2,2)
C     DIMENSION DMDKY(2,2),DADDM(2,2),DADKX(2,2),DADKY(2,2)
C     CALL DMDDR(OMEGA,AKX,AKY,C,VX,VY,H,A,EM,DMDDM,DMDKX,DMDKY)
C
C                         ----EXTERNAL SUBROUTINES REQUIRED----
C
C     DADDR,CAI,SAI
C
C                         ----ARGUMENT LIST----
C
C     OMEGA       R*4     ND      INP
C     AKX         R*4     ND      INP
C     AKY         R*4     ND      INP
C     C           R*4     ND      INP
C     VX          R*4     ND      INP
C     VY          R*4     ND      INP
C     H           R*4     ND      INP
C     A           R*4     2-BY-2  INP
C     EM          R*4     2-BY-2  OUT
C     DMDDM       R*4     2-BY-2  OUT
C     DMDKX       R*4     2-BY-2  OUT
C     DMDKY       R*4     2-BY-2  OUT
C
C NO COMMON STORAGE USED
C
C                         ----INPUTS----
C
C     OMEGA       =ANGULAR FREQUENCY  RAD/SEC
C     AKX         =X COMPONENT OF HORIZONTAL WAVE NUMBER VECTOR IN 1/KM
C     AKY         =Y COMPONENT OF HORIZONTAL WAVE NUMBER VECTOR IN 1/KM
C     C           =SOUND SPEED IN KM/SEC
C     VX          =X COMPONENT OF WIND VELOCITY IN KM/SEC
C     VY          =Y COMPONENT OF WIND VELOCITY IN KM/SEC
C     H           =THICKNESS IN KM OF LAYER
C     A(I,J)      =(I,J)-TH ELEMENT OF MATRIX A FOR UHS
C
C                         ----OUTPUTS----
C
C     EM          =2-BY-2 TRANSFER MATRIX WHICH RELATES THE SOLUTIONS
C                  OF THE RESIDUAL EQUATIONS AT THE TOP OF A LAYER
```

```
C                    TO THOSE AT THE BOTTOM OF THE LAYER.
C     DMDDM(I,J)  =(I,J)-TH ELEMENT OF MATRIX DMDDM
C     DMDKX(I,J)  =(I,J)-TH ELEMENT OF MATRIX DMDKX
C     DMDKY(I,J)  =(I,J)-TH ELEMENT OF MATRIX DMDKY
C
C                        ----PROGRAM FOLLOWS BELOW----
C
      SUBROUTINE DMDDR(OMEGA,AKX,AKY,C,VX,VY,H,A,EM,DMDDM,DMDKX,DMDKY)
      DIMENSION EM(2,2),DMDX(2,2),DMDDM(2,2),DMDKX(2,2),DMDKY(2,2)
      DIMENSION A(2,2),DADDM(2,2),DADKX(2,2),DADKY(2,2)
      CALL DADDR(OMEGA,AKX,AKY,C,VX,VY,DADDM,DADKX,DADKY)
      HSQ=H*H
      X=(A(1,1)**2+A(1,2)*A(2,1))*HSQ
      CA=CAI(X)
      SA=SAI(X)
      DCAIX=0.5*SA
      Y=ABS(X)
      IF(Y-1.0E-2) 3,3,4
    3 DSAIX=1.0-X/60.0+X**2/1680.0+X**3/90720.0
      GO TO 5
    4 DSAIX=0.5*(CA-SA)/X
    5 GEM=H*DSAIX
      DO 20 I=1,2
      DO 20 J=1,2
   20 DMDX(I,J)=-GEM*A(I,J)
      DO 30 I=1,2
   30 DMDX(I,I)=DMDX(I,I)+DCAIX
      DXDDM=(2.0*A(1,2)*DADDM(1,1)+A(1,2)*DADDM(2,1)+A(2,1)*DADDM(1,2))*
     1HSQ
      DXDKX=(2.0*A(1,1)*DADKX(1,1)+A(1,2)*DADKX(2,1)+A(2,1)*DADKX(1,2))*
     1HSQ
      DXDKY=(2.0*A(1,1)*DADKY(1,1)+A(1,2)*DADKY(2,1)+A(2,1)*DADKY(1,2))*
     1HSQ
      T=H*SA
      DO 90 I=1,2
      DO 90 J=1,2
      DMDDM(I,J)=DMDX(I,J)*DXDDM-T*DADDM(I,J)
      DMDKX(I,J)=DMDX(I,J)*DXDKX-T*DADKX(I,J)
      DMDKY(I,J)=DMDX(I,J)*DXDKY-T*DADKY(I,J)
   90 EM(I,J)=-T*A(I,J)
      DO 190 I=1,2
  190 EM(I,I)=EM(I,I)+CA
      RETURN
      END
```

```
C     DRDDR (SUBROUTINE)  MODIFIED  7/11/74  LAST CARD IN DECK IS NO.
C
C
C                    ----ABSTRACT----
C
C TITLE - DRDDR
C         THE PURPOSE OF THIS SUBROUTINE IS TO COMPUTE THE COMPONENTS
C         OF THE MATRICES DRDDM, DRDKX, AND DRDKY WHICH REPRESENT THE
C         PARTIAL DERIVATIVES OF THE RPP MATRIX WHICH WOULD BE
C         COMPUTED BY SUBROUTINE RRRR.
C                  DRDDM IS THE PARTIAL DERIVATIVE MATRIX OF RPP WRT OMEGA
C                  DRDKX IS THE PARTIAL DERIVATIVE MATRIX OF RPP WRT AKX
C                  DRDKY IS THE PARTIAL DERIVATIVE MATRIX OF RPP WRT AKY
C
C LANGUAGE - FORTRAN V (UNIVAC 1108, REFERENCE MANUAL UP-7536 REV. 1)
C AUTHORS - A.D. PIERCE, CHRISTOPHER KAPPER, G.I.T., JULY, 1974
C
C                    ----CALLING SEQUENCE----
C
C SEE SUBROUTINE COMPK
      DIMENSION CI(100),VXI(100),VYI(100),HI(100)
      DIMENSION RPP(2,2),A(2,2),DRDDM(2,2),DRDKX(2,2),DRDKY(2,2)
      DIMENSION EM(2,2),DMDDM(2,2),DMDKX(181),DMDKY(2,2)
      DIMENSION UPP(2,2),DPP(2,2),AINT(2,2)
      COMMON IMAX,CI,VXI,VYI,HI
      CALL DRDDR(OMEGA,AKX,AKY,RPP,A,DRDDM,DRDKX,DRDKY)
C
C                    ----EXTERNAL SUBROUTINES REQUIRED----
C
C     DMDDR (DMDDR CALLS DADDR,CAI,SAI)
C
C                    ----ARGUMENT LIST----
C
C     OMEGA       R*4    NO     INP
C     AKX         R*4    NO     INP
C     AKY         R*4    NO     INP
C     RPP         R*4    2-BY-2 INP
C     A           R*4    2-BY-2 INP
C     DRDDM       R*4    2-BY-2 OUT
C     DRDKX       R*4    2-BY-2 OUT
C     DRDKY       R*4    2-BY-2 OUT
C
C COMMON STORAGE USED
C     COMMON IMAX,CI,VXI,VYI,HI
C
C     IMAX        I*4    NO     INP
C     CI          R*4    100    INP
C     VXI         R*4    100    INP
C     VYI         R*4    100    INP
C     HI          R*4    100    INP
C
C                    ----INPUTS----
C
C     OMEGA       =ANGULAR FREQUENCY  RAD/SEC
C     AKX         =X COMPONENT OF HORIZONTAL WAVE NUMBER VECTOR IN 1/KM
C     AKY         =Y COMPONENT OF HORIZONTAL WAVE NUMBER VECTOR IN 1/KM
C     RPP         =2-BY-2 TRANSFER MATRIX WHICH CONNECTS SOLUTIONS
C                  OF THE RESIDUAL EQUATIONS AT THE BOTTOM OF THE
C                  UPPER HALFSPACE TO SOLUTIONS AT THE GROUND.
C     A           =MATRIX A OF COEFFICENTS
C
C                    ----OUTPUTS----
```

```
C
C     DRDOM(I,J)  =(I,J)-TH ELEMENT OF MATRIX DRDOM
C     DRDKX(I,J)  =(I,J)-TH ELEMENT OF MATRIX DRDKX
C     DRDKY(I,J)  =(I,J)-TH ELEMENT OF MATRIX DRDKY
C
C                        ----PROGRAM FOLLOWS BELLOW----
C
      SUBROUTINE DRDQR(OMEGA,AKX,AKY,RPP,A,DRDOM,DRDKX,DRDKY)
      DIMENSION CI(100),VXI(100),VYI(100),HI(100)
      DIMENSION RPP(2,2),A(2,2),DRDOM(2,2),DRDKX(2,2),DRDKY(2,2)
      DIMENSION EM(2,2),DMDOM(2,2),DMDKX(2,2),DMDKY(2,2)
      DIMENSION DPP(2,2),DPP(2,2),AINT(2,2)
      COMMON IMAX,CI,VXI,VYI,HI
      DO 10 I=1,2
      DO 10 J=1,2
      DRDOM(I,J)=0.0
      DRDKX(I,J)=0.0
   10 DRDKY(I,J)=0.0
      DPP(1,1)=1.0
      DPP(1,2)=0.0
      DPP(2,1)=0.0
      DPP(2,2)=1.0
      DO 15 I=1,2
      DO 15 J=1,2
   15 DPP(I,J)=RPP(I,J)
      DO 100 J=1,IMAX
      I=IMAX+1-J
      C=CI(I)
      VX=VXI(I)
      VY=VYI(I)
      H=HI(I)
      CALL DMDQR(OMEGA,AKX,AKY,C,VX,VY,H,A,EM,DMDOM,DMDKX,DMDKY)
C     MULTIPLY DPP TIMES THE INVERSE OF EM
      AINT(1,1)=DPP(1,1)*EM(2,2)-DPP(1,2)*EM(2,1)
      AINT(1,2)=-DPP(1,1)*EM(1,2)+DPP(1,2)*EM(1,1)
      AINT(2,1)=DPP(2,1)*EM(2,2)-DPP(2,2)*EM(2,1)
      AINT(2,2)=-DPP(2,1)*EM(1,2)+DPP(2,2)*EM(1,1)
      DO 20 II=1,2
      DO 20 JJ=1,2
   20 DPP(II,JJ)=AINT(II,JJ)
      DO 30 II=1,2
      DO 30 JJ=1,2
      DO 30 KK=1,2
      DO 30 LL=1,2
      DRDOM(II,JJ)=DRDOM(II,JJ)+DPP(II,KK)*DMDOM(KK,LL)*UPP(LL,JJ)
      DRDKX(II,JJ)=DRDKX(II,JJ)+DPP(II,KK)*DMDKX(KK,LL)*UPP(LL,JJ)
   30 DRDKY(II,JJ)=DRDKY(II,JJ)+DPP(II,KK)*DMDKY(KK,LL)*UPP(LL,JJ)
      DO 40 II=1,2
      DO 40 JJ=1,2
   40 AINT(II,JJ)=EM(II,1)*UPP(1,JJ)+EM(II,2)*UPP(2,JJ)
      DO 50 II=1,2
      DO 50 JJ=1,2
   50 UPP(II,JJ)=AINT(II,JJ)
  100 CONTINUE
      RETURN
      END
```

APPENDIX B

UTILITY PROGRAM FOR DETERMINING THE SIGN OF REAL AND IMAGINARY PARTS OF THE EIGENMODE DISPERSION FUNCTION

This program determines the sign of the real and imaginary parts of the eigenmode dispersion function for a specified search range of the real and imaginary parts of the complex horizontal wave number. The quantities G^2, ω_{AU}, and ω_{BU} are as defined previously. In the deck listing a L on the end of a computer variable refers to the lower layer of the two layer atmosphere while a U designates the upper halfspace. This program performs its calculations in double precision and in explicit complex variable notation using an array technique where the array positions 1 and 2 represent the real and imaginary parts of the respective complex variable. For the purpose of computing the sign of the real and imaginary parts of the eigenmode dispersion function the following equations are defined

$$X^2 = ([\omega_{AL}^2-\omega^2]/c_L^2 + [\omega^2-\omega_{BL}^2]k^2/\omega^2)H^2 \qquad (B\text{-}1)$$

where H is the distance to the bottom of the upper halfspace. The quantities A_{11} and A_{12} are as defined in Section 2.1

noting that for this model there are no horizontal winds. From Pierce[8] we have the functions and equations

$$CAI(X) = \cosh(X) \tag{B-2a}$$

$$SAI(X) = \sinh(X)/(X) \tag{B-2b}$$

$$R_{11} = CAI(X) - (H)SAI(X) \tag{B-3}$$

$$R_{12} = (-H)(A_{12L})SAI(X) \tag{B-4}$$

where there is no ambiguity regarding the sign of X determined from X^2 because the functions CAI and SAI are constructed to facilitate both cases. With these equations and the upper boundary condition the computer program computes the sign of the real and imaginary parts of the eigenmode dispersion function as per Eqs. (2.16) and (2.23).

The inputs for this program are the wind speeds in the lower and upper atmosphere depicted respectively by CL and CU. A value for ω is chosen along with a horizontal and vertical range for the array described by variables NR and NI. The inputs AKRL, AKRU, AKIL, and AKIU describe the lower and upper bounds for the search region for real and imaginary k. The height H is as described before. When the input integer IOPT is positive, the output presented in this paper is obtained. When IOPT is negative values for OMEGA, AKR,

and AKI along with the values for the real and imaginary parts of the eigenmode dispersion function can be printed out for any number of rows desired.

When running the program, the listing in this Appendix produces the arrays for branch I. By reversing the signs of GU(1) and GU(2) after line 34 in subroutine CNMDFN branch II can be explored.

```
      C MAIN PROGRAM
            DIMENSION DORN(100),STOR(100)
            NAMELIST /NAM1/ CL,CU,OMEGA,NR,NI,AKRL,AKRU,AKIL,AKIU,H,IOPT
            DATA Q2/1H+/
            DATA Q3/1H-/
            READ (5,NAM1)
            DELTR=(AKRU-AKRL)/(NR-1)
            DELTI=(AKIU-AKIL)/(NI-1)
            AKI=AKIU
            WRITE (6,12)
         12 FORMAT (1H1,5X)
            DO 100 I=1,NI
            DO 50 J=1,NR
            AKR=AKRL+(J-1)*DELTR
            CALL CNMDFN(OMEGA,AKR,AKI,CL,CU,H,RNMD,AINMD)
            IF (IOPT .GE. 0) GO TO 29
            WRITE (6,23) OMEGA,AKR,AKI,RNMD,AINMD
         23 FORMAT (1H ,6HOMEGA=,F13.8,3X,4HAKR=,F13.8,3X,4HAKI=,F13.8,3X,6HNM
           1DFN=,G13.8,3X,2H+I,G13.8)
         29 CONTINUE
            IF (RNMD) 31,31,33
         31 DORN(J)=Q3
            GO TO 35
         33 DORN(J)=Q2
         35 CONTINUE
         50 CONTINUE
            WRITE (6,71) AKI,(DORN(J),J=1,NR)
         71 FORMAT (1H ,F14.10,3X,100A1)
            AKI=AKI-DELTI
        100 CONTINUE
            DO 110 I=1,NR
        110 STOR(I)=AKRL+(I-1)*DELTR
            WRITE (6,115) OMEGA,(STOR(I),I=1,NR)
        115 FORMAT (1H ,6HOMEGA=,F13.9,3X,4HAKR=,(5F11.7))
            WRITE (6,118)
        118 FORMAT (1H1,35HSIGN OF THE IMAGINARY PART OF NMDFN)
            AKI=AKIU
            DO 200 I=1,NI
            DO 150 J=1,NR
            AKR=AKRL+(J-1)*DELTR
            CALL CNMDFN(OMEGA,AKR,AKI,CL,CU,H,RNMD,AINMD)
            IF (IOPT .GE. 0) GO TO 129
            WRITE (6,23) OMEGA,AKR,AKI,RNMD,AINMD
        129 CONTINUE
            IF (AINMD) 131,131,133
        131 DORN(J)=Q3
            GO TO 135
        133 DORN(J)=Q2
        135 CONTINUE
        150 CONTINUE
            WRITE (6,171) AKI,(DORN(J),J=1,NR)
        171 FORMAT (1H ,F14.10,3X,100A1)
            AKI=AKI-DELTI
        200 CONTINUE
            DO 210 I=1,NR
        210 STOR(I)=AKRL+(I-1)*DELTR
            WRITE (6,215) OMEGA,(STOR(I),I=1,NR)
        215 FORMAT (1H ,6HOMEGA=,F13.9,3X,4HAKR=,(5F11.7))
            END
```

```
      SUBROUTINE CNMOFN(OMEGA,AKR,AKI,CL,CU,H,RNMD,AINMD)
      DOUBLE PRECISION GUSQ(2),XSQ(2),A11U(2),A12U(2),X(2),GU(2)
      DOUBLE PRECISION A11L(2),A12L(2),R11(2),R12(2),CAIX(2),SAIX(2)
      DOUBLE PRECISION OMAU,OMAL,OMBU,OMBL,A,B,C,D,E,F,PH1,PH2
      GRAV =.0098D0
      GAMMA=1.400
      OMAU=GAMMA*GRAV/(2.0*CU)
      OMAL=GAMMA*GRAV/(2.0*CL)
      OMBU=DSQRT(GAMMA-1.0)*GRAV/CU
      OMBL=DSQRT(GAMMA-1.0)*GRAV/CL
      GUSQ(1)=(OMAU**2-OMEGA**2)/(CU**2)+((OMEGA**2-OMBU**2)*(AKR**2
     1-AKI**2))/(OMEGA**2)
      GUSQ(2)=(2.0*AKR*AKI*(OMEGA**2-OMBU**2))/(OMEGA**2)
      XSQ(1)=(OMAL**2-OMEGA**2)/(CL**2)+((OMEGA**2-OMBL**2)*(AKR**2
     1-AKI**2))/(OMEGA**2)
      XSQ(2)=(2.0*AKR*AKI*(OMEGA**2-OMBL**2))/(OMEGA**2)
      XSQ(1)=XSQ(1)*H**2
      XSQ(2)=XSQ(2)*H**2
      A11U(1)=((GRAV*(AKR**2-AKI**2))/(OMEGA**2))-(GAMMA*GRAV)/(2.0
     1*CU**2)
      A11U(2)=(2.0*AKR*AKI*GRAV)/(OMEGA**2)
      A12U(1)=1-((CU**2)*(AKR**2-AKI**2))/(OMEGA**2)
      A12U(2)=(-2.0*AKR*AKI*(CU**2))/(OMEGA**2)
      A=GUSQ(1)**2
      B=GUSQ(2)**2
      C=DSQRT(A+B)
      C=DSQRT(C)
      CALL PHASE(GUSQ,PH1)
      GU(1)=C*(DCOS(PH1/2.0))
      GU(2)=C*(DSIN(PH1/2.0))
      IF (GU(1) .GE. 0.0) GO TO 10
      GU(1)=-GU(1)
      GU(2)=-GU(2)
   10 CONTINUE
      D=XSQ(1)**2
      E=XSQ(2)**2
      F=DSQRT(D+E)
      F=DSQRT(F)
      CALL PHASE(XSQ,PH2)
      X(1)=F*(DCOS(PH2/2.0))
      X(2)=F*(DSIN(PH2/2.0))
      CAIX(1)=DCOS(X(2))*DCOSH(X(1))
      CAIX(2)=DSIN(X(2))*DSINH(X(1))
      SAIX(1)=(X(1)*DCOS(X(2))*DSINH(X(1))+X(2)*DSIN(X(2))*DCOSH(X(1)))/
     1(X(1)**2+X(2)**2)
      SAIX(2)=(X(1)*DSIN(X(2))*DCOSH(X(1))-X(2)*DCOS(X(2))*DSINH(X(1)))/
     1(X(1)**2+X(2)**2)
      A11L(1)=((GRAV*(AKR**2-AKI**2))/(OMEGA**2))-(GAMMA*GRAV)/(2.0*CL
     1**2)
      A11L(2)=(2.0*AKR*AKI*GRAV)/(OMEGA**2)
      A12L(1)=1-((CL**2)*(AKR**2-AKI**2))/(OMEGA**2)
      A12L(2)=(-2.0*AKR*AKI*(CL**2))/(OMEGA**2)
      R11(1)=CAIX(1)-H*SAIX(1)*A11L(1)+H*SAIX(2)*A11L(2)
      R11(2)=CAIX(2)-H*A11L(2)*SAIX(1)-H*SAIX(2)*A11L(1)
      R12(1)=-H*SAIX(1)*A12L(1)+H*SAIX(2)*A12L(2)
      R12(2)=-H*SAIX(1)*A12L(2)-H*SAIX(2)*A12L(1)
      RNMD=A12U(1)*R11(1)-A12U(2)*R11(2)-R12(1)*GU(1)-R12(1)*A11U(1)
     1+GU(2)*R12(2)+A11U(2)*R12(2)
      AINMD=A12U(1)*R11(2)+A12U(2)*R11(1)-GU(2)*R12(1)-R12(1)*A11U(2)
     1-GU(1)*R12(2)-R12(2)*A11U(1)
      RETURN
      END
```

```
1*          SUBROUTINE PHASE(GUSQ,PH1)
2*          DOUBLE PRECISION GUSQ(2),PH1
3*          IF (GUSQ(1) .LE. 0.0) GO TO 5
4*          IF (GUSQ(2) .LE. 0.0) GO TO 7
5*          PH1=DATAN(GUSQ(2)/GUSQ(1))
6*          GO TO 9
7*        5 IF (GUSQ(2) .LE. 0.0) GO TO 6
8*          PH1=3.14159265358D0-DATAN(-GUSQ(2)/GUSQ(1))
9*          GO TO 9
10*       6 PH1=3.14159265358D0+DATAN(GUSQ(2)/GUSQ(1))
11*         GO TO 9
12*       7 PH1=-DATAN(-GUSQ(2)/GUSQ(1))
13*       9 CONTINUE
14*         RETURN
15*         END
```

BIBLIOGRAPHY

1. Pierce, A. D., and J. W. Posey, Theoretical Prediction of Acoustic-Gravity Pressure Waveforms Generated by Large Explosions in the Atmosphere, Air Force Cambridge Research Laboratories Report AFCRL-70-0134, 1970.

2. Pierce, A. D., C. A. Moo and J. W. Posey, Generation and Propagation of Infrasonic Waves, Air Force Cambridge Research Laboratories Report AFCRL-TR-73-0135, 1973.

3. Pierce, A. D., "Propagation of Acoustic-Gravity Waves in a Temperature- and Wind-Stratified Atmosphere," J. Acoust. Soc. Amer. 37, 219 (1965).

4. Pierce, A. D., J. W. Posey and E. F. Iliff, "Variation of Nuclear Explosion Generated Acoustic-Gravity Wave Forms with Burst Height and with Energy Yield," J. Geophys. Res. 76, 5025-5042 (1971).

5. Pierce, A. D., Infrasonic Modes: An Omnibus Digital Computer Program for the Study of Acoustic-Gravity Wave Propagation, Avco Corp., AFCRL-66-669, AVSSD-0230-66-CR, Sci. Rep. 6, (5 September 1966).

6. Donn, W. L. and D. M. Shaw, "Exploring the Atmosphere with Nuclear Explosions," Rev. of Geophys. 5, 53-82 (1967).

7. Brune, J. N., J. E. Nate and L. E. Alsop, "The Polar Phase Shift of Surface Waves on a Sphere," Bull. Seism. Soc. Amer. 51, 247-257 (1961).

8. Pierce, A. D., "The Multilayer Approximation for Infrasonic Wave Propagation in a Temperature- and Wind-Stratified Atmosphere," J. Comp. Phys. 1, 343-359 (1967).